Molecular Immunology 54 (2013) 238–246

Contents lists available at SciVerse ScienceDirect

Molecular Immunology

journal homepage: www.elsevier.com/locate/molimm

Analysis of genetic and predisposing factors in Japanese patients with atypical hemolytic uremic syndrome

Xinping Fan[a,1], Yoko Yoshida[b], Shigenori Honda[a], Masanori Matsumoto[b], Yugo Sawada[c], Motoshi Hattori[d], Shuichi Hisanaga[e], Ryosuke Hiwa[f], Fumihiko Nakamura[g], Maiko Tomomori[h], Shinichiro Miyagawa[h], Rika Fujimaru[i], Hiroshi Yamada[i], Toshihiro Sawai[j], Yuhachi Ikeda[j], Naoyuki Iwata[k], Osamu Uemura[k], Eiji Matsukuma[l], Yoshiaki Aizawa[m], Hiroshi Harada[n], Hideo Wada[o], Eiji Ishikawa[p], Akira Ashida[q], Masaomi Nangaku[r], Toshiyuki Miyata[a,*], Yoshihiro Fujimura[b,**]

[a] *Department of Molecular Pathogenesis, National Cerebral and Cardiovascular Center, Suita, Japan*
[b] *Department of Blood Transfusion Medicine, Nara Medical University, Kashihara, Japan*
[c] *Department of Urology, Tokyo Women's Medical University, Tokyo, Japan*
[d] *Department of Pediatric Nephrology, Tokyo Women's Medical University, Tokyo, Japan*
[e] *Department of Internal Medicine, Koga General Hospital, Miyazaki, Japan*
[f] *Department of General Internal Medicine, Tenri Hospital, Tenri, Japan*
[g] *Department of Hematology, Tenri Hospital, Tenri, Japan*
[h] *Department of Pediatrics, National Hospital Organization Kure Medical Center, Kure, Japan*
[i] *Department of Pediatrics, Osaka City General Hospital, Osaka, Japan*
[j] *Department of Pediatrics, Shiga University of Medical Science, Otsu, Japan*
[k] *Department of Pediatric Nephrology, Aichi Children's Health and Medical Center, Obu, Japan*
[l] *Department of Pediatrics, Gifu Prefectural General Medical Center, Gifu, Japan*
[m] *Department of Internal Medicine, Iwamizawa Municipal General Hospital, Iwamizawa, Japan*
[n] *Department of Kidney Transplant Surgery, Sapporo City General Hospital, Sapporo, Japan*
[o] *Department of Molecular and Laboratory Medicine, Mie University Graduate School of Medicine, Tsu, Japan*
[p] *Department of Cardiology and Nephrology, Mie University Graduate School of Medicine, Tsu, Japan*
[q] *Department of Pediatrics, Osaka Medical College, Takatsuki, Japan*
[r] *Division of Nephrology and Endocrinology, University of Tokyo School of Medicine, Tokyo, Japan*

ARTICLE INFO

Article history:
Received 5 November 2012
Accepted 9 December 2012

Keywords:
Alternative pathway of complement system
Atypical hemolytic uremic syndrome
Complement factor
Genetic mutation

ABSTRACT

Hemolytic uremic syndrome (HUS) is characterized by microangiopathic hemolytic anemia, thrombocytopenia, and renal impairment. Approximately 10% of cases are classified as atypical due to the absence of Shiga toxin-producing bacteria as a trigger. Uncontrolled activation of the complement system plays a role in the pathogenesis of atypical HUS (aHUS). Although many genetic studies on aHUS have been published in recent years, only limited data has been gathered in Asian countries. We analyzed the genetic variants of 6 candidate genes and the gene deletion in complement factor H (CFH) and CFH-related genes, examined the prevalence of CFH autoantibodies and evaluated the genotype-phenotype relationship in 10 Japanese patients with aHUS. We identified 7 causative or potentially causative mutations in *CFH* (p.R1215Q), *C3* (p.R425C, p.S562L, and p.I1157T), membrane cofactor protein (p.Y189D and p.A359V) and thrombomodulin (p.T500M) in 8 out of 10 patients. All 7 of the mutations were heterozygous and four of them were novel. Two patients carried *CFH* p.R1215Q and 3 other patients carried *C3* p.I1157T. One patient had 2 causative mutations in different genes. One patient was a compound heterozygote of the 2 *MCP* mutations. The patients carrying mutations in *CFH* or *C3* had a high frequency of relapse and a worse prognosis. One patient had CFH autoantibodies. The present study identified the cause of aHUS in 9

Abbreviations: aHUS, atypical hemolytic uremic syndrome; CFH, complement factor H; C3, complement component 3; MCP, membrane cofactor protein; CFI, complement factor I; CFB, complement factor B; CFD, complement factor D; THBD, thrombomodulin; CFHRs, CFH related genes; SCR, short consensus repeat; RCA, regulators of complement activation; RFLP, restriction fragment length polymorphism; MLPA, multiplex ligation-dependent probe amplification; URTI, upper respiratory tract infection.

* Corresponding author at: Department of Molecular Pathogenesis, National Cerebral and Cardiovascular Center, 5-7-1 Fujishirodai, Suita, Osaka 565-8565, Japan. Tel.: +81 6 6833 5012; fax: +81 6 6835 1176.
** Corresponding author at: Department of Blood Transfusion Medicine, Nara Medical University, 840 Shijo-cho, Kashihara, Nara, 634-8521, Japan. Tel: +81 074 422 3051; fax: +81 074 429 0771.
E-mail addresses: miyata@ri.ncvc.go.jp (T. Miyata), yoshifuji325@naramed-u.ac.jp (Y. Fujimura).
[1] Permanent address: Department of Clinical Laboratory, Beijing Chaoyang Hospital, Capital Medical University, Beijing, China

0161-5890/$ – see front matter
http://dx.doi.org/10.1016/j.molimm.2012.12.006

out of 10 Japanese patients. Since the phenotype-genotype correlation of aHUS has clinical significance in predicting renal recovery and transplant outcome, a comprehensively accurate assessment of molecular variation would be necessary for the proper management of aHUS patients in Japan.

1. Introduction

Hemolytic uremic syndrome (HUS) is characterized by microangiopathic hemolytic anemia, thrombocytopenia, and renal impairment (Boyce et al., 1995). Approximately 10% of the cases are classified as atypical due to the absence of Shiga toxin-producing bacteria infection as a trigger (Noris and Remuzzi, 2009). Compared to typical HUS, atypical HUS (aHUS, OMIM #235400) has a much poorer prognosis, with up to half of the patients progressing to end-stage renal disease, and a higher mortality (Tarr et al., 2005).

The alternative pathway of the complement system is a natural defense system against invasive microbial attack, in which complement component C3 (C3), the central complement protein, is hydrolyzed to C3b and directly binds to the microbe for opsonization or for the subsequent activation of the complement pathway (Roumenina et al., 2011). When C3b binds to the host cells, the further activation of the complement system is stringently limited by several endogenous complement regulatory proteins which are present on the surface of the host cells (Sethi & Fervenza, 2012). Complement factor H (CFH) and membrane cofactor protein (MCP or CD46) are the regulators in the complement pathway. Both proteins can accelerate the complement factor I (CFI)-mediated proteolytic inactivation of C3b and C4b. CFH can also inhibit the formation of the C3 convertase, C3bBb, by competing with complement factor B (CFB) for binding to C3b and thereby accelerate the decay of C3bBb simultaneously (Roumenina et al., 2011; Sethi and Fervenza, 2012). Thrombomodulin, an endothelial anticoagulant glycoprotein encoded by *THBD*, also functions as a cofactor for the CFI-mediated C3b inactivation, and mutations of *THBD* predispose to aHUS (Delvaeye et al., 2009).

Maintenance of the complement system involves a balance between activation and regulation. Uncontrolled activation of the alternative pathway of the complement system plays a role in the pathogenesis of aHUS. More than half of the patients with aHUS have mutations of genes involved in the alternative pathway of the complement system (Noris and Remuzzi, 2009). Mutations with loss-of-function of regulators (*CFH, CFI, MCP*, and *THBD*) (Delvaeye et al., 2009; Noris et al., 2010; Richards et al., 2003; Sellier-Leclerc et al., 2007) and gain-of-function of key complement components (*C3* and *CFB*) (Fremeaux-Bacchi et al., 2008; Goicoechea de Jorge et al., 2007) have been found to predispose to aHUS. In addition, genomic deletions in the regulators of complement activation (RCA) located on chromosome 1q32 are reportedly associated with the occurrence of aHUS due to the high homology among *CFH* and 5 CFH-related genes (*CFHR3, CFHR1, CFHR4, CFHR2*, and *CFHR5* lie in tandem at 1q32) (Zipfel et al., 2007). In particular, deletion of *CFHR3* and *CFHR1* as a result of non-allelic homologous recombination has been linked to a risk of aHUS (Venables et al., 2006), sometimes together with the presence of CFH autoantibodies (Jozsi et al., 2008; Skerka et al., 2009).

A normal plasma level of complement proteins does not preclude the presence of a mutation in these genes. More importantly, genotype–phenotype correlations of aHUS have clinical significance in predicting renal recovery and transplant outcome (Noris et al., 2010). Therefore, it is important to perform genetic screening of these genes in patients with aHUS. In this study, we described the clinical phenotypes in 10 Japanese aHUS patients, sequenced the 6 candidate genes *CFH, MCP, CFI, C3, CFB*, and *THBD*, examined the gene deletion of *CFH* and *CFHR*s in the RCA region, evaluated the penetrance of genetic abnormalities, and finally determined the genotype–phenotype correlations.

2. Materials and methods

2.1. Patients

Ten Japanese patients with aHUS were investigated in this study; 8 of them were sporadic and the other two were from one family. Diagnosis of aHUS was defined by the simultaneous occurrence of microangiopathic hemolytic anemia, thrombocytopenia, and acute renal failure without association to Shiga toxin (Ariceta et al., 2009). Clinical events preceding the acute HUS episode were recorded. Laboratory data were collected. The study was approved by the Institutional Review Board of each institution. Written informed consent was obtained from all of the participants.

2.2. Complement analyses

Serum C3 and C4 levels were measured by nephelometry. The CFH antigen level was determined by a rocket-immunoelectrophoresis method using pooled plasma of healthy individuals as 100%. The normal ranges of C3, C4, and CFH were 86–160 mg/dl, 14–49 mg/dl, and 50–150%, respectively.

2.3. ADAMTS13 activity assay

ADAMTS13 activity was measured by a chromogenic ADAMTS13-act-ELISA using a glutathione-conjugated VWF73 peptide as the substrate (Kato et al., 2006).

2.4. Hemolytic assay

Resuspended sheep red blood cells (Japan Lamb, Japan) were incubated with a dilution series of a patient plasma sample at 37 °C for 30 min, and the level of hemoglobin release from the red blood cells was measured by the absorbance at 414 nm (A_{414}) (Sanchez-Corral et al., 2004). The absorbance obtained from the addition of an excess amount of a neutralizing antibody against CFH was defined as 100%. The characterization of the neutralizing antibody against CFH will be described elsewhere. The hemolysis activity of the patients was expressed as the percentage obtained using A_{414} taken from the patient to that obtained using the neutralizing antibody against CFH. A value of more than 50% was regarded as apparent hemolysis.

2.5. Autoantibody against CFH

The autoantibody was examined by the Western blot method(Moore et al., 2010). Purified CFH was electrophoresed on a 5% SDS–polyacrylamide gel and transferred to a polyvinylidene fluoride membrane. After blocking with 5% dried milk, the membrane was cut into 0.5-cm wide strips and each strip was incubated with the 100-fold diluted patient plasma sample overnight at 4 °C. Horseradish peroxidase-labeled goat anti-human IgG antibody was used as the secondary antibody and bound autoantibodies were visualized by an enhanced chemiluminescence substrate (Western Lightning-ECL, PerkinElmer, Japan).

2.6. Mutation screening

Genomic DNA was extracted using a QIAamp DNA Blood Mini Kit (Qiagen, Germany) from peripheral blood leukocytes of patients and their family members. The coding exons and the intronic flanking regions of *CFH* (NM_000186.3), *C3* (NM_000064.2), *MCP* (NM_002389.4), *CFI* (NM_000204.3), *CFB* (NM_001710.5) and *THBD* (NM_000361.2) were amplified by the polymerase chain reaction. The sequences of gene-specific primers and the polymerase chain reaction conditions are listed in Supplementary Table 1. A routine sequencing reaction was carried out in both directions. The A of the ATG translation initiation start site was designated as position +1 and the initial Met was denoted as +1. The potential pathogenicity of missense mutations was examined by several programs for predicting the functional significance of missense mutations; these were PolyPhen-2 (http://genetics.bwh.harvard.edu/pph2/), AGVGD (http://agvgd.iarc.fr/cgi-bin/agvgd_output.cgi), SIFT (http://sift.jcvi.org/www/SIFT_enst_submit.html) and PMut (http://mmb.pcb.ub.es/PMut/).

2.7. Restriction fragment length polymorphism (RFLP) analysis

The RFLP analysis was applied for confirmation of mutations in the family members. The amplified DNA fragments were digested with a restriction enzyme (New England Biolabs, USA) (Table 1). The digests were electrophoresed to determine the genotypes according to the cleaved bands.

2.8. Screening for gene deletions

Multiplex ligation-dependent probe amplification (MLPA) analysis was used to screen the gene deletions in the RCA region on chromosome 1q32 using a commercially available kit (MLPA kit P236-A2; MRC-Holland, the Netherlands). The relative dosage ratio was calculated by Coffalyser v9.4. The probe ratios of deletions should be below 0.7.

3. Results

The clinical features and laboratory data of the 10 patients with aHUS are summarized in Table 2. The parents of all patients were non-consanguineous. Plasma ADAMTS13 activity was within the range of 29–119% in all patients. All the patients showed no signs for infection of Shiga toxin-producing *Escherichia coli*. The first episode of aHUS occurred at childhood (≤10 yr) in 7 patients. Nine cases had probable triggering events. The plasma C3 level was low in patients X1, GG1, HH1 and JJ1. The plasma C4 and CFH levels were in the normal range except in the case of patient HH1, who exhibited a mild decrease in C4. Patients X1, GG1, and II1 showed apparent hemolytic activity against the sheep erythrocytes. The presence of CFH autoantibody was confirmed in only one patient (GG1) (Fig. 1). Five patients had experienced relapses by the most recent follow-up. Five patients progressed to end-stage renal disease and could not be maintained without hemodialysis or peritoneal dialysis.

DNA sequencing of 6 candidate genes identified 17 missense mutations in 10 aHUS patients (Table 2). We considered that 3 of the missense mutations were causative for aHUS, 4 of the novel missense mutations were potentially causative, as described in the results of each proband, and the remaining 10 missense mutations were likely neutral. The detailed characteristics of causative or potentially causative mutations are summarized in Table 3. All of the causative or potentially causative mutations were heterozygous. The causative mutations in the family members were confirmed by the RFLP analysis and were inherited from their unaffected father or mother (Fig. 2). Gene deletions of *CFH* and *CFHR*s in the RCA region were not found in any of the aHUS probands by the MLPA analysis (Table 2).

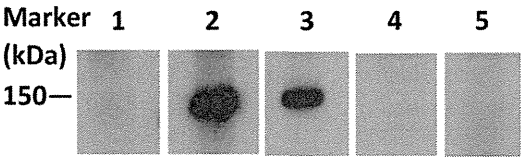

Fig. 1. Detection of CFH autoantibody in family GG. Purified CFH was electrophoresed on a 5% SDS–polyacrylamide gel and transferred to the polyvinylidene fluoride membrane. The membrane was cut into 0.5-cm wide strips and incubated with the diluted plasma sample. Horseradish peroxidase-labeled goat anti-human IgG antibody was used to detect the bound autoantibody. Lane 1, CFH autoantibody-negative plasma; lane 2, CFH autoantibody-positive plasma; lane 3, plasma from patient GG1; lane 4, plasma from patient GG1's father; lane 5, plasma from patient GG1's mother.

3.1. Patient X1

In this male patient, the initial presentation of aHUS was observed after episodes of vomiting, diarrhea and hematuria at 22 years of age (Table 2). At that time, he progressed to anuria. He was treated with hemodialysis three times per week together with drug therapy. At 30 years of age he received a live relative kidney transplantation, but at only 3 weeks after transplantation a renal biopsy of the allograft showed evidence of thrombotic microangiopathy, indicating aHUS had recurred. He received plasma exchanges five times in a week and then gradually tapered to once every two weeks. He is now undergoing treatment with eculizumab, a recombinant humanized monoclonal antibody that specifically binds to complement protein C5, preventing the generation of the cytotoxic membrane-attack complex, C5b-9. Currently, his creatinine level is mildly elevated (2.0–2.5 mg/dl, equal to 177–221 μmol/L).

He had a causative mutation, p.R1215Q, in the short consensus repeats (SCR) 20 domain of *CFH*. He inherited this mutation from his unaffected father (Tables 2 and 3, Fig. 2). Both the patient and his father showed apparently enhanced hemolytic activity.

3.2. Patient AA1

This male patient showed his first overt clinical signs of thrombotic microangiopathy with some petechiae on the face and body at 3 years of age after a cold (Table 2). Then he experienced 6 recurrences of aHUS at the ages of 9, 15, 18, 22, and 29 (twice), with each of these episodes being triggered by upper respiratory tract infection (URTI) or influenza A virus. At the first bout, when he was 29 years old, his laboratory data were improved after 4 plasma exchanges. At the second bout triggered by influenza A, his renal function was worse than that in the first instance, so he was treated with 12 plasma exchanges and 5 rounds of hemodialysis. In each case, his renal function was recovered by prompt treatment after onset.

He had a causative mutation p.I1157T in the thioester-containing domain of *C3*. His unaffected father was a heterozygote for this mutation (Tables 2 and 3, Fig. 2). His hemolytic activity was not enhanced.

3.3. Patient CC1

This male patient developed aHUS at 4 years of age after URTI with palpebral edema and ecchymosis on both his legs and buttocks. He obtained a complete remission only by routine and supportive treatment (Table 2). No causative mutations were identified in the 6 genes sequenced. His hemolytic activity was not enhanced.

Table 1
Restriction fragment length polymorphism (RFLP) assay for causative or potentially causative mutations.

Gene	Reference sequence	Exon	Amino acid change	Restriction enzyme[a]	Allele cut	Forward primer (5′-3′)	Reverse primer (5′-3′)
CFH	NM_000186.3	23	R1215Q	HpyCH4 V	1215Q	atccgtgtgtaatatcccgaga	gcacaagttggatactccagt
C3	NM_000064.2	12	R425C	Hha I	Wild-type	caattcccaggtctcaggga	gagagaaaaggagaaaggg
		13	S562L	Ban II	Wild-type	caattcccaggtctcaggga	gagagaaaaggagaaaggg
		27	I1157T	Ssp I	Wild-type	gcctttgttctcatctcgctgc-aggaggctaaaaata[b]	ctggggataataagagtgactt-acctttcaggctgc
MCP	NM_002389.4	5	Y189D	Sfc I	Wild-type	gtgaagtagaagtatttgagta-tcttgatgcagtaacc[b]	gatgaaactatttacaaaatgttt-ccatagtatttacaaatg
		12	A359V	HpyCH4 V	Wild-type	ggggagttggatttagatagca	ggtaggacaaactaatgcaggc
THBD	NM_000361	1	T500M	BsaH I	Wild-type	cactgctaccctaactacgacct	taaggtgctttggtagcaaagctg

[a] All of the restriction enzymes were available from New England Biolabs (MA, USA) and we used the reaction conditions recommended by the instructions.
[b] The underlined bases in the primer were mismatched with the wild-type sequence in order to introduce the restriction enzyme site.

3.4. Patient DD1

This male patient developed aHUS at 6 years of age, triggered by infection with influenza A virus (Table 2). He had clear thrombocytopenia (platelet count, 20×10^9/L) and hemolytic anemia (hemoglobin, 10 g/dL; lactate dehydrogenase, 3884 U/L) with schistocytes. His creatinine level was 0.9 mg/dL, equal to 79.6 mmol/L on admission, and it increased to 2.85 mg/dL, equal to 251.9 mmol/L. It is noteworthy that neurological abnormalities were also detected. His serological indexes were recovered after treatment with consecutive plasma exchange for 3 days and continuous hemodiafiltration for 7 days.

He had a causative mutation p.Y189D in the SCR3 domain of *MCP* and a potentially causative mutation p.A359V in the transmembrane region of *MCP*. His father and his younger brother had the p.Y189D mutation and his mother had the p.A359V mutation (Tables 2 and 3, Fig. 2). Therefore, the proband was a compound heterozygote for the p.Y189D and p.A359V mutations in *MCP*. None of the family members except for the proband showed any signs of aHUS. His hemolytic activity was not enhanced.

3.5. Patient FF1

This female patient was diagnosed with aHUS at 2 years of age after initial symptoms of palpebral edema and ecchymosis on both her legs appeared. Anemia and thrombocytopenia were improved by transfusion of erythrocyte concentrate and platelets. Her renal function could not be maintained without hemodialysis at that time. She has been treated with peritoneal dialysis for 2 years since her discharge.

She had a potentially causative mutation p.S562L in the β chain of *C3*. The unaffected mother and younger brother carried this mutation (Tables 2 and 3, Fig. 2). Her hemolytic activity was not enhanced.

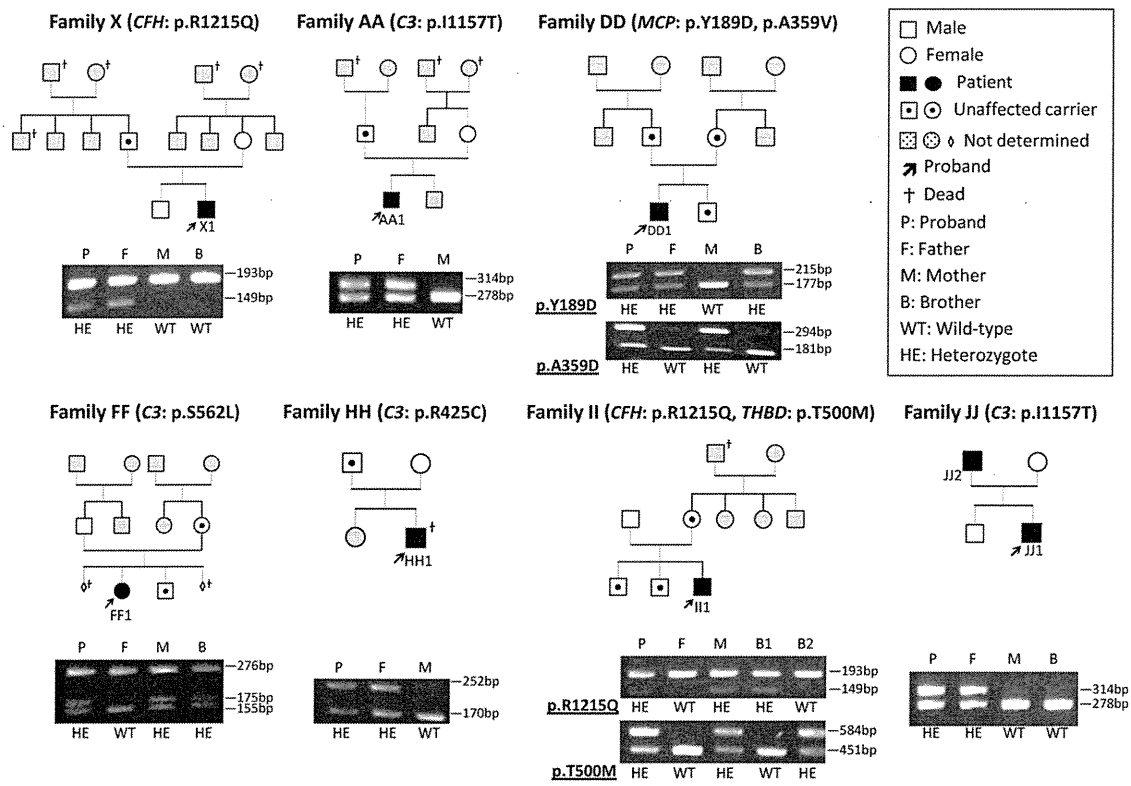

Fig. 2. Family pedigree of 8 patients with aHUS carrying causative or potentially causative mutations. Restriction fragment length polymorphism (RFLP) analyses of causative or potentially causative mutations are shown. The wild-type (WT) and heterozygote (HE) are distinguished by the electrophoretogram after digestion with the corresponding restriction enzyme. The size of bands is labeled.

Table 2
Clinical characteristics and genetic variations of 10 patients with aHUS.

Patient		X1	AA1	CC1	DD1	FF1	GG1	HH1	111	JJ1	JJ2
Gender		M	M	M	M	F	F	M	M	M	M
Age of first episode		22y	9y	4y	6y	2y	5y	8m	28y	2y	70y
Period of follow-up		9y	21y	~1y	~1y	2y	~1y	1m	2y	34y	1y
Probable triggering events		URTI	URTI	URTI	Influenza A virus	None	Viral gastroenteritis	Surgery	Gastroenteritis	URTI	Surgery
C3 (mg/dl)[a]		55.9	110	123	111	110.8	67	40	109	58.5	NA
C4 (mg/dl)[a]		18.3	40.6	22	28	29.2	26	12.7	45	40.8	NA
CFH antigen (%)[a]		97	118	98	75	98	66	75	125	122	104
Hemolytic assay		+	–	–	–	–	+	–	+	±	±
Treatment		PE, HD, eculizumab	PE, HD	conservative	PE, HD	HD, PD	PE, FFP	HD, FFP	PE, HD, FFP	PE, HD	HD
Relapse (number)		1	5	0	0	0	0	0	1	7	1
Transplantation (number)		1	0	0	0	0	0	0	0	0	0
Outcome currently		ESRD	Complete remission[b]	Complete remission[b]	Complete remission[b]	ESRD	Complete remission[b]	Dead	ESRD	ESRD	ESRD
Missense mutations[c]											
CFH	c.184G>A	p.V62I	p.V62I	p.V62I		p.V62I	p.V62I		p.V62I		
	c.1204T>C[d]	p.Y402H	p.Y402H	p.Y402H	p.Y402H						
	c.2509G>A										p.V837I
	c.2808G>T	p.E936D				p.E936D	p.E936D	p.E936D(homo)	p.E936D	p.E936D	p.E936D
	c.3644G>A	**p.R1215Q**							**p.R1215Q**		
MCP	c.38C>T	p.S13F									
	c.565T>G				**p.Y189D**						
	c.1076C>T				**p.A359V**						
CFI	c.603A>C							p.R201S		p.R201S	p.R201S
	c.1217G>A				p.R406H						
C3	c.1273C>T							**p.R425C**			
	c.1685C>T					**p.S562L**					
	c.3470T>C		**p.I1157T**							**p.I1157T**	**p.I1157T**
CFB	c.94C>T									p.R32W	p.R32W(homo)
	c.95G>A	p.R32Q			p.R32Q				p.R32Q		
THBD	c.1418C>T	p.A473V	p.A473V(homo)	p.A473V	p.A473V		p.A473V	p.A473V	p.A473V		
	c.1499C>T								**p.T500M**		
CNV of CFH and CFHRs		Normal	Normal	Normal	Normal	Normal	Normal	Normal	Normal	Normal	Normal

Abbreviations: y, year; m, month; CFH, complement factor H; MCP, membrane cofactor protein; CFI, complement factor I; C3, complement component 3; CFB, complement factor B; THBD, thrombomodulin; CFHRs, CFH related genes; URTI, upper respiratory tract infection; NA, not available; PE, plasma exchange; HD, hemodialysis; PD, peritoneal dialysis; FFP, fresh frozen plasma; ESRD, end-stage renal disease; CNV, copy number variation; homo, homozygote.

[a] Normal range: C3, 86–160 mg/dL; C4, 14–49 mg/dL; CFH, 50–150%.

[b] Complete remission is defined as normalization of both hematologic parameters (hematocrit > 30%; hemoglobin > 10 g/dL; lactate dehydrogenase < 460 U/L; platelet count > 150,000/μL) and renal function (serum creatinine < 1.3 mg/dL, equal to 114.92 μmol/L).

[c] Bold and underlined, definitely causative mutation; Bold, novel and potentially causative mutation; The A of the ATG of the initial Met codon is denoted as nucleotide +1, and the initial Met residue is denoted as amino acid +1.

[d] Reference sequence of CFH (NM 000186.3) is c.1204C>T.

Table 3
Detailed characteristics of the causative or potentially causative mutations.

Gene	Mutation identified		Change in nucleotide	Domain	Location in 3D model	Prediction in silico[a]				Conservative[b]	Reported (Ref.)	Family	Genotype			
	Precursor	Mature				PolyPhen2	AGVGD	SIFT	PMut				Proband	Father	Mother	Brother
CFH	p.R1215Q	p.R1197Q	c.3644 G>A	SCR20	Exposed	Probably damaging	Likely interfere with function	Tolerated	Neutral	Yes	Reported (18,22)	X II	HE HE	HE WT	WT HE	WT 1:HE; 2: WT
C3	p.R425C	p.R403C	c.1273C>T	MG4	Exposed	Possible damaging	Most likely interfere with function	Damaging	Pathological	No	Novel	HH	HE	HE	WT	-
	p.S562L	p.S540L	c.1685C>T	MG6	Buried	Benign	Most likely interfere with function	Damaging	Neutral	No	Novel	FF	HE	WT	HE	HE
	p.I1157T	p.I1135T	c.3470 T>C	TED	Exposed	Benign	Most likely interfere with function	Tolerated	Neutral	Yes	Reported (17,19)	AA JJ	HE HE	HE HE	WT WT	– WT
MCP	p.Y189D	p.Y155D	c.565 T>G	SCR3	Buried	Probably damaging	Most likely interfere with function	Damaging	Neutral	Yes	Reported (20)	DD	HE	HE	WT	HE
	p.A359V	p.A325V	c.1076C>T	TM	–	Benign	Most likely interfere with function	Tolerated	Pathological	No	Novel	DD	HE	WT	HE	WT
THBD	p.T500M	p.T482M	c.1499C>T	STRD	–	Possible damaging	Most likely interfere with function	Tolerated	Pathological	Yes	Novel	II	HE	WT	HE	1: WT; 2:HE

Abbreviations: CFH, complement factor H; C3, complement component 3; MCP, membrane cofactor protein; THBD, thrombomodulin; SCR, short consensus repeat; MG, macroglobulin-like domain; TED, thioester-containing domain; TM, transmembrane region; STRD, serine and threonine-rich domain; HE, Heterozygote; WT, wild-type.

[a] The corresponding websites were described in the text.

[b] If more than 75% of the aligned species share the same amino acid, this amino acid is defined as conservative (i.e. yes).

3.6. Patient GG1

This female patient was the second of three children, but her elder sister was dead because of hemorrhagic shock at birth. Her father is Caucasian and her mother is Japanese. At 5 years of age, she presented with aHUS triggered by viral gastroenteritis with jaundice and ecchymosis on the trunk as the first manifestation. She received 12 plasma exchanges and methylprednisolone for 3 consecutive days, after which her laboratory tests were normal.

We did not identify a causative mutation or deletion of *CFH* or *CFH*-related genes (Table 2). But the CFH autoantibodies were detected by Western blot (lane 3 in Fig. 1). Both this patient and her unaffected father were positive in the hemolytic assay and the lysis activity was corrected by the addition of purified CFH (Table 2).

3.7. Patient HH1

This male patient was diagnosed with aHUS at 8 months of age, one month after his surgery for tetralogy of Fallot. After diagnosis, his condition deteriorated rapidly and he died within about 4 weeks despite being treated with fresh frozen plasma infusions and hemodialysis (Table 2).

He had a potentially causative mutation p.R425C in the β chain of *C3* (Tables 2 and 3, Fig. 2). His unaffected father had this mutation. His hemolytic activity was not enhanced.

3.8. Patient II1

This male patient had experienced several epileptic seizures in his teenage years. At 28 years of age, he developed HUS with extremely low platelet count (9×10^9/L) and rather severe renal dysfunction (creatinine, 13–14 mg/dL, equal to 1149–1238 μmol/L) (Table 2). His laboratory data were improved after treatment with fresh frozen plasma infusions for 1 day, 12 plasma exchanges and 4 weeks of hemodialysis. After discharge from the hospital 4 months later, he had a relapse. Renal biopsy revealed glomerular thrombotic microangiopathies. His renal function did not recover, although he was still being treated with hemodialysis at the most recent follow-up date.

He had the causative mutation p.R1215Q in *CFH* and one potentially causative mutation p.T500M in *THBD* (Tables 2 and 3, Fig. 2). His unaffected mother was a heterozygote for both mutations. Both he and his mother were positive in the hemolytic assay (Table 2).

3.9. Patients JJ1 and JJ2

Patient JJ1 was a male patient who developed aHUS at the age of 2. He then experienced 5 recurrences of aHUS before the age of 10 years (Table 2). At the age of 10, he was treated with peritoneal dialysis for acute renal failure. At 33 years of age, he again presented with HUS triggered with URTI. His laboratory data were improved after the 25th hemodialysis treatment. He had another recurrence of aHUS one year later. Treatments with 18 rounds of hemodialysis and plasma exchange were performed but the latter was interrupted because of anaphylactic shock. Patient JJ2, the father of patient JJ1, developed aHUS after his nephrectomy at 70 years of age. He was then treated with antiplatelet and antihypertensive agents, but 1 year and 3 months later, he developed acute renal failure with epileptic seizures and pulmonary edema. He was treated with hemodialysis at that time, but his renal function has been getting worse.

Both patients JJ1 and JJ2 carried the causative mutation p.I1157T in *C3* (Tables 2 and 3, Fig. 2). Both showed mildly elevated hemolytic activities (Table 2).

4. Discussion

In the present study, we identified 7 causative or potentially causative mutations in 8 of 10 Japanese patients with aHUS and the presence of CFH autoantibodies in another patient. Three of the mutations, p.R1215Q in *CFH*, p.I1157T in *C3*, and p.Y189D in *MCP*, were identified previously (Caprioli et al., 2006; Fremeaux-Bacchi et al., 2006; Maga et al., 2010; Martínez-Barricarte et al. 2008; Mukai et al., 2011), indicating that these mutations are causative for aHUS. The remaining 4 missense mutations, p.A359V in *MCP*, p.S562L and p.R425C in *C3*, and p.T500M in *THBD*, were novel. We considered them as potentially causative mutations based on the available information, including prediction programs, a search of the literature, and the position of the missense mutation in the three-dimensional structure, as described below. No causative mutations in *CFI* and *CFB* were detected and no genetic rearrangements in the RCA region were observed.

CFH, a principal regulator of the complement system, is composed of 20 SCRs. Several ligands, including C3b, C3d, heparin, and cell surface glycosaminoglycans, can bind to SCR19–20 in CFH (Manuelian et al., 2003). We identified the p.R1215Q mutation located in SCR20 of CFH in 2 aHUS patients who showed increased hemolytic activities. Functional analysis of a mutant CFH with p.R1215Q revealed reduced heparin-binding ability with a normal binding capacity for C3b, C3d, and the endothelial surface through glycosaminoglycans (Kajander et al., 2011; Morgan et al., 2011). This mutation has previously been reported in 3 Japanese aHUS patients in 2 families (Mukai et al., 2011). In the present study we identified it in 5 Japanese individuals, including 2 aHUS patients in 2 independent families. Therefore, the p.R1215Q mutation in *CFH* may be spread throughout the Japanese population.

C3 plays a major role in the complement system. In the present study, 5 aHUS patients carried 3 different missense mutations, p.R425C, p.S562L, and p.I1157T, in *C3*. Two mutations, p.R425C and p.S562L, are novel and the p.I1157T mutation has previously been reported in the United States and Spain (Maga et al., 2010; Martínez-Barricarte et al., 2008). The p.I1157T mutation was present in the thioester-containing domain, a hot area for C3 mutation. Mutagenesis studies revealed that the p.I1157A mutation in C3d attenuated the CFH19–20 binding by a factor of 4–6 when compared to wild-type C3d (Morgan et al., 2011). In addition, Ile1157 is an important contacting residue for complement receptor 2 (Clemenza and Isenman, 2000). Thus, we conclude that the p.I1157T mutation is causative. Two other novel mutations, p.R425C and p.S562L, are present in the macroglobulin 4 or 6 domain of the β chain in C3, respectively, and would be positioned on the surface of this domain based on the crystal structure (Janssen et al., 2005). More than two programs predicted that the p.R425C mutation was "Possibly damaging" or "Pathological" (Table 3). The p.S562L mutation occurred at the site close to the previously reported aHUS mutations, p.R592Q and p.R592W, which showed an impaired binding to the regulator protein, MCP (Fremeaux-Bacchi et al., 2008). Thus, we regarded them as potentially causative mutations.

MCP, a membrane-bound complement regulator highly expressed on most cell surfaces, acts as a cofactor for the CFI-mediated degradation of C3b and C4b (Lublin et al., 1988). The 4 extracellular SCRs are the binding site for C3b. Patient DD1 was a compound heterozygote for the p.Y189D and p.A359V mutations and developed aHUS after infection with influenza A-type virus, strongly indicating the precipitation of the hereditary and environmental risk factors for aHUS. In a French aHUS cohort, a heterozygous p.Y189D mutation was found in 3 out of 120 patients, 2 of whom were siblings (Fremeaux-Bacchi et al., 2006). The mutant MCP with the p.Y189D mutation led to a misfolded protein and an impaired function (Fremeaux-Bacchi et al., 2006). Therefore, we regarded p.Y189D as a causative mutation. The other mutation, p.A359V, was novel. This mutation occurred at the site close to the previously reported mutation, p.A353V (p.A304V in the previous reports), which has been identified in patients with aHUS and/or preeclampsia (Fang et al., 2008; Salmon et al., 2011). The p.A353V mutation had a defective ability to control the activation of the complement alternative pathway on a cell surface (Fang et al., 2008). In our study, only the proband carrying both the p.Y189D and p.A359V mutations developed aHUS, while the family members carrying only one of these mutations did not. The p.A359V mutation would modify the development of aHUS.

Mutations in thrombomodulin, a transmembrane endothelial glycoprotein encoded by *THBD*, accounted for the etiology in 3–5% of the aHUS patients (Delvaeye et al., 2009; Maga et al., 2010). The p.T500M mutation identified in patient II1 was located in the Ser- and Thr-rich region of thrombomodulin. Next to it, the p.P501L mutation was identified in an aHUS patient and exhibited defects in suppressing activation of the alternative complement pathway *in vitro* (Delvaeye et al., 2009). Moreover, three kinds of prediction in silico indicated that the p.T500M mutation was "Possibly damaging" or "Pathological" (Table 3). Considering this data together, we regarded this mutation as potentially causative and implicated in the pathogenesis of aHUS.

The CpG dinucleotide is a mutation hot spot and about 23% of single base-pair substitutions are CG → TG or CG → CA transitions, a frequency 5-fold higher than that for mutations in other dinucleotides (Krawczak et al., 1998). Among the 7 causative or potentially causative mutations, 4 mutations, p.R1215Q in *CFH*, p.S562L and p.R425C in *C3*, and p.T500M in *THBD*, occurred at the CpG dinucleotide.

Other synonymous and nonsynonymous SNPs were also identified in our patients (Table 2). Although these common variants are not extremely destructive, their pathogenic roles cannot be ignored, especially when combined (Heurich et al., 2011). The risk variant of *CFH* 402H weakened the CFH binding to sialylated surfaces (Herbert et al., 2007; Prosser et al., 2007), whereas the protective variant *CFH* 62I directly influenced the complement alternative pathway activity through a stronger binding to C3b and by acting as a better cofactor of CFI (Tortajada et al., 2009). The other protective variant *CFB* 32Q showed a reduction in C3bBb complex formation (Montes et al., 2009). Further "risk" combinations (*CFH* 62V/*CFB* 32R) resulted in a 2-fold increase in alterative pathway activation compared with the "protective" variants (*CFH* 62I/*CFB* 32Q) (Tortajada et al., 2009). All of the above-mentioned risk alleles were identified in our patients, half of whom were carriers of two or three "risk" alleles (Table 2). Therefore, the additive effects must dramatically exceed the effects of any single allele. A more comprehensive understanding of these disease-associated genetic variants is required.

Hemolytic assays are frequently used to evaluate the function of CFH (Heinen et al., 2006; Sanchez-Corral et al., 2004). Generally, the plasma samples containing the mutations in the C-terminal domains of CFH would show increased hemolytic activity. In our study, 2 aHUS patients with the *CFH* p.R1215Q mutation and the unaffected carriers in their families showed increased hemolytic activity, as did the other patient (GG1) with CFH autoantibodies.

Among the 7 patients carrying mutations in *CFH* or *C3* in the present study, one died and the remaining 5 patients progressed to end-stage renal disease. Patient AA1 obtained complete remission (Table 2). Five of 7 patients had a relapse. In contrast, one patient, DD1, the compound heterozygote for 2 mutations in *MCP*, had a better prognosis of complete remission without a relapse. These results obtained in Japanese aHUS patients were consistent with those obtained in Westerners (Loirat & Fremeaux-Bacchi, 2011). The overall midterm prognosis of aHUS is poor. At the first episode or within one year after onset, 50–70% or 60% of patients carrying the *CFH* or *C3* mutations, respectively, either died or reached

end-stage renal disease (Loirat & Fremeaux-Bacchi, 2011; Noris et al., 2010). Therefore, genetic information in patients with aHUS would be highly valuable for prognosis.

Incomplete penetrance of aHUS in the mutation carriers in the family has previously been reported (Caprioli et al., 2006; Loirat & Fremeaux-Bacchi, 2011; Noris et al., 2010). The present study confirmed this observation in Japanese aHUS patients (Fig. 2). The identified mutations were inherited from the patients' unaffected fathers or mothers. The single exception was a patient (JJ1) whose father (JJ2) had aHUS. None of the proband's siblings with the same mutation developed aHUS. It is likely that mutations do not directly cause an aHUS phenotype but rather modify the phenotype or predispose an individual to aHUS. The environmental factors and/or other genetic variations as a second hit are required for the manifestations of aHUS on one main genetic background (Francis et al., 2012; Pickering et al., 2007). Indeed, the onset of the disease was associated with infection or surgery in 9 out of 10 patients in our study (Table 2).

Patient X1 with the *CFH* p.R1215Q mutation received a live kidney transplantation, but failed three weeks later with recurrent aHUS. This result was consistent with the previous observations that the risk of post-transplant aHUS relapse is rather high in patients with *CFH* mutations (Loirat and Fremeaux-Bacchi, 2011; Noris & Remuzzi, 2009). In contrast, a lower risk of recurrence was reported in patients with the *MCP* mutation (Noris et al., 2010). One of the reasons for this variability is that CFH is a plasma protein synthesized by the liver, whereas MCP is synthesized by each cell locally. Therefore, combined liver–kidney transplantation might sometimes be a better option for CFH–associated patients based on a consideration of the risks/benefits in the individual patient (Saland et al., 2009). However, it should be noted that a relative kidney donor is not recommended, especially for patients with the *MCP* mutation, considering the possibly similar genetic background (Loirat and Fremeaux-Bacchi, 2011). Correspondingly, plasma exchange and plasma infusion may be a better and more logical choice for patients with the *CFH* mutation, but not efficient for correction of the essential defect in patients with MCP mutations, at least in theory.

In summary, the prevalence of genetic variation was evaluated in 10 Japanese aHUS patients. Seven causative or potentially causative mutations were identified in *CFH, C3, MCP*, and *THBD* in 8 patients and another patient was a carrier of CFH autoantibodies. The relationship between the genotype and phenotype was analyzed. Since the phenotype-genotype correlation of aHUS has clinical significance in predicting renal recovery and transplant outcome, a comprehensively accurate assessment of molecular variation would facilitate the clinical management for aHUS patients in Japan.

Conflict of interest

Dr. Fujimura is on the clinical advisory boards for Baxter Bioscience and Alexion Pharmaceuticals. Drs. Matsumoto, Hattori, and Ashida are on the clinical advisory board for Alexion Pharmaceuticals.

Contributions

T. Miyata and Y. Fujimura designed the study. X.P. Fan performed the genetic analysis with the guidance of S. Honda. Y. Yoshida and M. Matsumoto performed the protein analysis and hemolytic assay. Y. Yoshida, M. Matsumoto, Y. Sawada, M. Hattori, S. Hisanaga, R. Hiwa, F. Nakamura, M. Tomomori, S. Miyagawa, R. Fujimaru, H. Yamada, T. Sawai, Y. Ikeda, N. Iwata, O. Uemura, E. Matsukuma, Y. Aizawa, H. Harada, H. Wada, E. Ishikawa, A. Ashida, and M. Nangaku contributed to the sample collection, clinical data acquisition and interpretation of the data. X.P. Fan, T. Miyata, and Y. Fujimura interpreted the data and wrote the manuscript. All authors critically reviewed the manuscript.

Acknowledgements

This work was supported in part by grants-in-aid from the Ministry of Health, Labor, and Welfare of Japan, and Takeda Science Foundation. We thank Dr. Masashi Akiyama for structural modeling. The research activity of X.P. Fan, who is from Beijing Chaoyang Hospital affiliated with the Capital Medical University of China, was supported by a Scholarship from the Takeda Science Foundation.

Appendix A. Supplementary data

Supplementary Table 1

Appendix B. Supplementary data

Supplementary data associated with this article can be found, in the online version, at http://dx.doi.org/10.1016/j.molimm.2012.12.006.

References

Ariceta, G., Besbas, N., Johnson, S., Karpman, D., Landau, D., Licht, C., Loirat, C., Pecoraro, C., Taylor, C.M., Van de Kar, N., Vandewalle, J., Zimmerhackl, L.B., 2009. Guideline for the investigation and initial therapy of diarrhea-negative hemolytic uremic syndrome. Pediatric Nephrology 24, 687–696.

Boyce, T.G., Swerdlow, D.L., Griffin, P.M., 1995. Escherichia coli O157:H7 and the hemolytic-uremic syndrome. New England Journal of Medicine 333, 364–368.

Caprioli, J., Noris, M., Brioschi, S., Pianetti, G., Castelletti, F., Bettinaglio, P., Mele, C., Bresin, E., Cassis, L., Gamba, S., Porrati, F., Bucchioni, S., Monteferrante, G., Fang, C.J., Liszewski, M.K., Kavanagh, D., Atkinson, J.P., Remuzzi, G., 2006. Genetics of HUS: the impact of *MCPCFH*, and *IF* mutations on clinical presentation, response to treatment, and outcome. Blood 108, 1267–1279.

Clemenza, L., Isenman, D.E., 2000. Structure-guided identification of C3d residues essential for its binding to complement receptor 2 (CD21). Journal of Immunology 165, 3839–3848.

Delvaeye, M., Noris, M., De Vriese, A., Esmon, C.T., Esmon, N.L., Ferrell, G., Del-Favero, J., Plaisance, S., Claes, B., Lambrechts, D., Zoja, C., Remuzzi, G., Conway, E.M., 2009. Thrombomodulin mutations in atypical hemolytic-uremic syndrome. New England Journal of Medicine 361, 345–357.

Fang, C.J., Fremeaux-Bacchi, V., Liszewski, M.K., Pianetti, G., Noris, M., Goodship, T.H., Atkinson, J.P., 2008. Membrane cofactor protein mutations in atypical hemolytic uremic syndrome (aHUS), fatal Stx-HUS, C3 glomerulonephritis, and the HELLP syndrome. Blood 111, 624–632.

Francis, N.J., McNicholas, B., Awan, A., Waldron, M., Reddan, D., Sadlier, D., Kavanagh, D., Strain, L., Marchbank, K.J., Harris, C.L., Goodship, T.H., 2012. A novel hybrid *CFH/CFHR3* gene generated by a microhomology-mediated deletion in familial atypical hemolytic uremic syndrome. Blood 119, 591–601.

Fremeaux-Bacchi, V., Miller, E.C., Liszewski, M.K., Strain, L., Blouin, J., Brown, A.L., Moghal, N., Kaplan, B.S., Weiss, R.A., Lhotta, K., Kapur, G., Mattoo, T., Nivet, H., Wong, W., Gie, S., Hurault de Ligny, B., Fischbach, M., Gupta, R., Hauhart, R., Meunier, V., Loirat, C., Dragon-Durey, M.A., Fridman, W.H., Janssen, B.J., Goodship, T.H., Atkinson, J.P., 2008. Mutations in complement C3 predispose to development of atypical hemolytic uremic syndrome. Blood 112, 4948–4952.

Fremeaux-Bacchi, V., Moulton, E.A., Kavanagh, D., Dragon-Durey, M.A., Blouin, J., Caudy, A., Arzouk, N., Cleper, R., Francois, M., Guest, G., Pourrat, J., Seligman, R., Fridman, W.H., Loirat, C., Atkinson, J.P., 2006. Genetic and functional analyses of membrane cofactor protein (CD46) mutations in atypical hemolytic uremic syndrome. Journal of the American Society of Nephrology 17, 2017–2025.

Goicoechea de Jorge, E., Harris, C.L., Esparza-Gordillo, J., Carreras, L., Arranz, E.A., Garrido, C.A., Lopez-Trascasa, M., Sanchez-Corral, P., Morgan, B.P., Rodriguez de Cordoba, S., 2007. Gain-of-function mutations in complement factor B are associated with atypical hemolytic uremic syndrome. Proceedings of the National Academy of Sciences of the United States of America 104, 240–245.

Heinen, S., Sanchez-Corral, P., Jackson, M.S., Strain, L., Goodship, J.A., Kemp, E.J., Skerka, C., Jokiranta, T.S., Meyers, K., Wagner, E., Robitaille, P., Esparza-Gordillo, J., Rodriguez de Cordoba, S., Zipfel, P.F., Goodship, T.H., 2006. De novo gene conversion in the RCA gene cluster (1q32) causes mutations in complement factor H associated with atypical hemolytic uremic syndrome. Human Mutation 27, 292–293.

Herbert, A.P., Deakin, J.A., Schmidt, C.Q., Blaum, B.S., Egan, C., Ferreira, V.P., Pangburn, M.K., Lyon, M., Uhrin, D., Barlow, P.N., 2007. Structure shows that a glycosaminoglycan and protein recognition site in factor H is perturbed by age-related

macular degeneration-linked single nucleotide polymorphism. Journal of the Biological Chemistry 282, 18960–18968.
Heurich, M., Martinez-Barricarte, R., Francis, N.J., Roberts, D.L., Rodriguez de Cordoba, S., Morgan, B.P., Harris, C.L., 2011. Common polymorphisms in C3, factor B, and factor H collaborate to determine systemic complement activity and disease risk. Proceedings of the National Academy of Sciences of the United States of America 108, 8761–8766.
Janssen, B.J., Huizinga, E.G., Raaijmakers, H.C., Roos, A., Daha, M.R., Nilsson-Ekdahl, K., Nilsson, B., Gros, P., 2005. Structures of complement component C3 provide insights into the function and evolution of immunity. Nature 437, 505–511.
Jozsi, M., Licht, C., Strobel, S., Zipfel, S.L., Richter, H., Heinen, S., Zipfel, P.F., Skerka, C., 2008. Factor H autoantibodies in atypical hemolytic uremic syndrome correlate with CFHR1/CFHR3 deficiency. Blood 111, 1512–1514.
Kajander, T., Lehtinen, M.J., Hyvarinen, S., Bhattacharjee, A., Leung, E., Isenman, D.E., Meri, S., Goldman, A., Jokiranta, T.S., 2011. Dual interaction of factor H with C3d and glycosaminoglycans in host-nonhost discrimination by complement. Proceedings of the National Academy of Sciences of the United States of America 108, 2897–2902.
Kato, S., Matsumoto, M., Matsuyama, T., Isonishi, A., Hiura, H., Fujimura, Y., 2006. Novel monoclonal antibody-based enzyme immunoassay for determining plasma levels of ADAMTS13 activity. Transfusion 46, 1444–1452.
Krawczak, M., Ball, E.V., Cooper, D.N., 1998. Neighboring-nucleotide effects on the rates of germ-line single-base-pair substitution in human genes. American Journal of Human Genetics 63, 474–488.
Loirat, C., Fremeaux-Bacchi, V., 2011. Atypical hemolytic uremic syndrome. Orphanet Journal of Rare Diseases 6, 60.
Lublin, D.M., Liszewski, M.K., Post, T.W., Arce, M.A., Le Beau, M.M., Rebentisch, M.B., Lemons, L.S., Seya, T., Atkinson, J.P., 1988. Molecular cloning and chromosomal localization of human membrane cofactor protein (MCP). Evidence for inclusion in the multigene family of complement-regulatory proteins. Journal of Experimental Medicine 168, 181–194.
Maga, T.K., Nishimura, C.J., Weaver, A.E., Frees, K.L., Smith, R.J., 2010. Mutations in alternative pathway complement proteins in American patients with atypical hemolytic uremic syndrome. Human Mutation 31, E1445–E1460.
Manuelian, T., Hellwage, J., Meri, S., Caprioli, J., Noris, M., Heinen, S., Jozsi, M., Neumann, H.P., Remuzzi, G., Zipfel, P.F., 2003. Mutations in factor H reduce binding affinity to C3b and heparin and surface attachment to endothelial cells in hemolytic uremic syndrome. Journal of Clinical Investigation 111, 1181–1190.
Martínez-Barricarte, R., Montes, T., Pinto, S., Sánchez-Corral, P., López-Trascasa, M., Morgan, B.P., Harris, C.L., Córdoba, S.R.d., Novel C3 mutations associated with atypical haemolytic uraemic syndrome. Poster presented at: XXII International Complement Workshop 2008. Sep. 28-Oct. 2, 2008; Basel, Switzerland.
Montes, T., Tortajada, A., Morgan, B.P., Rodriguez de Cordoba, S., Harris, C.L., 2009. Functional basis of protection against age-related macular degeneration conferred by a common polymorphism in complement factor B. Proceedings of the National Academy of Sciences of the United States of America 106, 4366–4371.
Moore, I., Strain, L., Pappworth, I., Kavanagh, D., Barlow, P.N., Herbert, A.P., Schmidt, C.Q., Staniforth, S.J., Holmes, L.V., Ward, R., Morgan, L., Goodship, T.H., Marchbank, K.J., 2010. Association of factor H autoantibodies with deletions of CFHR1, CFHR3, CFHR4, and with mutations in *CFHCFICD46*, and *C3* in patients with atypical hemolytic uremic syndrome. Blood 115, 379–387.
Morgan, H.P., Schmidt, C.Q., Guariento, M., Blaum, B.S., Gillespie, D., Herbert, A.P., Kavanagh, D., Mertens, H.D., Svergun, D.I., Johansson, C.M., Uhrin, D., Barlow, P.N., Hannan, J.P., 2011. Structural basis for engagement by complement factor H of C3b on a self surface. Nature Structural and Molecular Biology 18, 463–470.
Mukai, S., Hidaka, Y., Hirota-Kawadobora, M., Matsuda, K., Fujihara, N., Takezawa, Y., Kubota, S., Koike, K., Honda, T., Yamauchi, K., 2011. Factor H gene variants in Japanese: its relation to atypical hemolytic uremic syndrome. Molecular Immunology 49, 48–55.
Noris, M., Caprioli, J., Bresin, E., Mossali, C., Pianetti, G., Gamba, S., Daina, E., Fenili, C., Castelletti, F., Sorosina, A., Piras, R., Donadelli, R., Maranta, R., van der Meer, I., Conway, E.M., Zipfel, P.F., Goodship, T.H., Remuzzi, G., 2010. Relative role of genetic complement abnormalities in sporadic and familial aHUS and their impact on clinical phenotype. Clinical Journal of the American Society of Nephrology 5, 1844–1859.
Noris, M., Remuzzi, G., 2009. Atypical hemolytic-uremic syndrome. New England Journal of Medicine 361, 1676–1687.
Pickering, M.C., de Jorge, E.G., Martinez-Barricarte, R., Recalde, S., Garcia-Layana, A., Rose, K.L., Moss, J., Walport, M.J., Cook, H.T., de Cordoba, S.R., Botto, M., 2007. Spontaneous hemolytic uremic syndrome triggered by complement factor H lacking surface recognition domains. Journal of Experimental Medicine 204, 1249–1256.
Prosser, B.E., Johnson, S., Roversi, P., Herbert, A.P., Blaum, B.S., Tyrrell, J., Jowitt, T.A., Clark, S.J., Tarelli, E., Uhrin, D., Barlow, P.N., Sim, R.B., Day, A.J., Lea, S.M., 2007. Structural basis for complement factor H linked age-related macular degeneration. Journal of Experimental Medicine 204, 2277–2283.
Richards, A., Kemp, E.J., Liszewski, M.K., Goodship, J.A., Lampe, A.K., Decorte, R., Muslumanoglu, M.H., Kavukcu, S., Filler, G., Pirson, Y., Wen, L.S., Atkinson, J.P., Goodship, T.H., 2003. Mutations in human complement regulator, membrane cofactor protein (CD46), predispose to development of familial hemolytic uremic syndrome. Proceedings of the National Academy of Sciences of the United States of America 100, 12966–12971.
Roumenina, L.T., Loirat, C., Dragon-Durey, M.A., Halbwachs-Mecarelli, L., Sautes-Fridman, C., Fremeaux-Bacchi, V., 2011. Alternative complement pathway assessment in patients with atypical HUS. Journal of Immunological Methods 365, 8–26.
Saland, J.M., Shneider, B.L., Bromberg, J.S., Shi, P.A., Ward, S.C., Magid, M.S., Benchimol, C., Seikaly, M.G., Emre, S.H., Bresin, E., Remuzzi, G., 2009. Successful split liver-kidney transplant for factor H associated hemolytic uremic syndrome. Clinical Journal of the American Society of Nephrology 4, 201–206.
Salmon, J.E., Heuser, C., Triebwasser, M., Liszewski, M.K., Kavanagh, D., Roumenina, L., Branch, D.W., Goodship, T., Fremeaux-Bacchi, V., Atkinson, J.P., 2011. Mutations in complement regulatory proteins predispose to preeclampsia: a genetic analysis of the PROMISSE cohort. PLoS Medicine 8, e1001013.
Sanchez-Corral, P., Gonzalez-Rubio, C., Rodriguez de Cordoba, S., Lopez-Trascasa, M., 2004. Functional analysis in serum from atypical Hemolytic Uremic Syndrome patients reveals impaired protection of host cells associated with mutations in factor H. Molecular Immunology 41, 81–84.
Sellier-Leclerc, A.L., Fremeaux-Bacchi, V., Dragon-Durey, M.A., Macher, M.A., Niaudet, P., Guest, G., Boudailliez, B., Bouissou, F., Deschenes, G., Gie, S., Tsimaratos, M., Fischbach, M., Morin, D., Nivet, H., Alberti, C., Loirat, C., 2007. Differential impact of complement mutations on clinical characteristics in atypical hemolytic uremic syndrome. Journal of the American Society of Nephrology 18, 2392–2400.
Sethi, S., Fervenza, F.C., 2012. Membranoproliferative glomerulonephritis–a new look at an old entity. New England Journal of Medicine 366, 1119–1131.
Skerka, C., Jozsi, M., Zipfel, P.F., Dragon-Durey, M.A., Fremeaux-Bacchi, V., 2009. Autoantibodies in haemolytic uraemic syndrome (HUS). Journal of Thrombosis and Haemostasis 101, 227–232.
Tarr, P.I., Gordon, C.A., Chandler, W.L., 2005. Shiga-toxin-producing *Escherichia coli* and haemolytic uraemic syndrome. Lancet 365, 1073–1086.
Tortajada, A., Montes, T., Martinez-Barricarte, R., Morgan, B.P., Harris, C.L., de Cordoba, S.R., 2009. The disease-protective complement factor H allotypic variant Ile62 shows increased binding affinity for C3b and enhanced cofactor activity. Human Molecular Genetics 18, 3452–3461.
Venables, J.P., Strain, L., Routledge, D., Bourn, D., Powell, H.M., Warwicker, P., Diaz-Torres, M.L., Sampson, A., Mead, P., Webb, M., Pirson, Y., Jackson, M.S., Hughes, A., Wood, K.M., Goodship, J.A., Goodship, T.H., 2006. Atypical haemolytic uraemic syndrome associated with a hybrid complement gene. PLoS Medicine 3, e431.
Zipfel, P.F., Edey, M., Heinen, S., Jozsi, M., Richter, H., Misselwitz, J., Hoppe, B., Routledge, D., Strain, L., Hughes, A.E., Goodship, J.A., Licht, C., Goodship, T.H., Skerka, C., 2007. Deletion of complement factor H-related genes *CFHR1* and *CFHR3* is associated with atypical hemolytic uremic syndrome. PLoS Genetics 3, e41.

Journal of Thrombosis and Haemostasis, **11**: 1399–1406 DOI: 10.1111/jth.12279

ORIGINAL ARTICLE

Crystal structure and enzymatic activity of an ADAMTS-13 mutant with the East Asian-specific P475S polymorphism

M. AKIYAMA,*[1] D. NAKAYAMA,*[1] S. TAKEDA,† K. KOKAME,* J. TAKAGI‡ and T. MIYATA*

**Department of Molecular Pathogenesis, National Cerebral and Cardiovascular Center; †Department of Cardiac Physiology, National Cerebral and Cardiovascular Center; and ‡Laboratory of Protein Synthesis and Expression, Institute for Protein Research, Osaka University, Osaka, Japan*

To cite this article: Akiyama M, Nakayama D, Takeda S, Kokame K, Takagi J, Miyata T. Crystal structure and enzymatic activity of an ADAMTS-13 mutant with the East Asian-specific P475S polymorphism. *J Thromb Haemost* 2013; **11**: 1399–406.

Summary. *Background:* An East Asian-specific P475S polymorphism in the gene encoding ADAMTS-13 causes an approximately 16% reduction in plasma ADAMTS-13 activity. *Objectives:* To demonstrate the impact of this dysfunctional polymorphism by characterizing the structure and activity of the P475S mutant protein. *Methods:* We determined the crystal structure of the P475S mutant of ADAMTS-13-DTCS (DTCS-P475S, residues 287–685) and compared it with the wild-type structure. We determined the enzymatic parameters of ADAMTS-13-MDTCS (residues 75–685) and MDTCS-P475S, and further examined the effects of denaturants and reaction temperature on their activity. We also examined the cleavage of shear-treated von Willebrand factor (VWF) by MDTCS-P475S. *Results:* MDTCS-P475S showed a reaction rate similar to that of wild-type MDTCS, but showed two-fold lower affinity for the peptidyl substrate, indicating that the Pro475-containing V-loop (residues 474–481) in the C_A domain is a substrate-binding exosite. Structural analysis showed that the conformation of the V-loop was significantly different in DTCS-P475S and the wild type, where no obvious interactions of Ser475 with other residues were observed. This explains the higher susceptibility of the enzymatic activity of MDTCS-P475S to reaction environments such as denaturants and high temperature. MDTCS-P475S can moderately cleave shear-treated VWF. *Conclusions:* We have provided structural evidence that the P475S polymorphism in ADAMTS-13 leads to increased local structural instability, resulting in lowered affinity for the substrate without changing the reaction rate. The moderate activity of ADAMTS-13-P475S for shear-treated VWF is sufficient to prevent thrombotic thrombocytopenic purpura (TTP) onset.

Keywords: ADAMTS-13, crystallography, genetic polymorphism, human, proteins, thrombotic thrombocytopenic purpura, von Willebrand factor.

Correspondence: Masashi Akiyama and Toshiyuki Miyata, Department of Molecular Pathogenesis, National Cerebral and Cardiovascular Center, 5-7-1 Fujishiro-dai, Suita, Osaka 565-8565, Japan.
Tel.: +81 6 6833 5012, ext: 2477 or 2512; fax: +81 6 6825 117.
E-mail: akiyamam@ri.ncvc.go.jp and miyata@ri.ncvc.go.jp

[1]These authors contributed equally to this work.

Received 11 October 2012
Manuscript handled by: D. Lane
Final decision: D. Lane, 5 April 2013

Introduction

von Willebrand factor (VWF) is a plasma glycoprotein synthesized primarily in vascular endothelial cells and megakaryocytes [1]. VWF is released into plasma as ultralarge multimeric forms (ultralarge VWF [UL-VWF]) that are highly active in platelet aggregation. ADAMTS-13 specifically cleaves the Tyr1605–Met1606 bond within the A2 domain of VWF in a fluid shear stress-dependent manner, and controls platelet thrombus formation [2,3]. Severe deficiency in ADAMTS-13 activity, caused by either genetic mutations or acquired autoantibodies against ADAMTS-13, results in the accumulation of UL-VWF in plasma, which leads to the hyperaggregation of platelets. This prothrombotic condition can cause thrombotic thrombocytopenic purpura (TTP) [4].

The human *ADAMTS13* gene encodes a precursor protein of 1427 amino acids with a modular structure consisting of a signal peptide, a propeptide, a metalloprotease (M) domain, a disintegrin-like (D) domain, a thrombospondin type 1 repeat (TSR) (T1), a cysteine-rich (C) domain, a spacer (S) domain, seven TSRs (T2–T8), and two CUB domains [5–7]. In addition to the causative mutations for TTP, a number of missense mutations and polymorphisms have been identified in *ADAMTS13* [6,8,9]. Among them, P475S (c.1423C>T) is a dysfunctional missense polymorphism with a minor allele frequency of 5.0% [8,10]. Subjects carrying the minor

allele residue (serine) showed ~ 16% lower ADAMTS-13 activity than those without the polymorphism. The P475S polymorphism has also been identified in Koreans (allele frequency of 4.0%) [11] and Chinese (1.5%) [12], but is absent in Caucasians [13], suggesting that ADAMTS-13-P475S is an East Asian-specific natural dysfunctional mutant [14]. An in vitro study demonstrated that ADAMTS-13-P475S is normally secreted from cultured cells. However, the culture medium containing ADAMTS-13-P475S showed greatly reduced enzymatic activity (~ 10%) in the VWF multimer assay [8]. On the other hand, partially purified ADAMTS-13-P475S showed ~ 70% of wild-type activity in an assay with a synthetic peptidyl fluorogenic substrate, FRETS-VWF73 [15]. The difference in enzymatic activity of ADAMTS-13-P475S between the two assays was probably attributable to the presence and absence of urea in the reaction mixture [15]. These experiments were performed with ADAMTS-13-containing culture medium or partially purified ADAMTS-13; therefore, analysis of enzyme kinetics with the purified protein remains to be performed.

Several studies have indicated that ADAMTS-13-MDTCS has VWF-cleaving activity that is nearly identical to that of full-length ADAMTS-13 in vitro [16,17]. We recently determined the crystal structures of ADAMTS-13-DTCS [18]. The C domain was further divided into the globular C_A domain and elongated C_B domain. Extensive structure-based mutagenesis indicated that ADAMTS-13 can bind to VWF through at least three VWF-binding exosites on the linearly aligned discontinuous surfaces of the D, C_A and S domains [18], and this substrate-binding mode with multiple binding sites is supported by other studies [19–22]. The Pro475 in question is located in the V-loop (residues 474–481) of the C_A domain. Mutations in the V-loop of the C_A domain resulted in significantly reduced enzymatic activity, suggesting that the V-loop creates a VWF-binding exosite [18].

In this study, we determined the crystal structure of DTCS-P475S, and characterized the enzymatic activity of MDTCS-P475S. The present study provides evidence that the P475S substitution in ADAMTS-13 destabilizes the local conformation of the V-loop in the C_A domain, resulting in lowered substrate affinity without changing the reaction rate. Furthermore, the moderate cleavage of shear-treated VWF by ADAMTS-13-P475S suggests that the VWF-cleaving activity of the mutant is sufficient to prevent TTP onset.

Materials and methods

Preparation, crystallization and structural analysis of DTCS-P475S

Production of DTCS-P475S was performed with a previously described method [23], with some modifications. Briefly, a stable cell line (HEK293S GnTI$^-$ cells) [24] secreting DTCS-P475S (residues 287–685) with a C-terminal tobacco etch virus (TEV) proteinase cleavage site followed by tandem His-tag sequences was selected and cultured. The culture medium was first concentrated with 50% (w/v) ammonium sulfate, and DTCS-P475S was purified by Ni^{2+}–nitrilotriacetic acid (NTA) agarose column chromatography (Sigma-Aldrich, St Louis, MO, USA). After digestion with TEV proteinase, DTCS-P475S was further purified with a Resource S cation-exchange column (GE Healthcare, Hatfield, UK), concentrated to 10 mg mL^{-1}, and crystallized in 20% (w/v) poly(ethylene glycol) 1500 and 100 mM Mes (pH 6.0), with the same method as described for wild-type DTCS [23]. The diffraction data were collected at the SPring-8 beamline BL38B1 by use of a Rayonix MX225HE CCD detector with a wavelength of 1.0 Å at 100 K. The structure of DTCS-P475S was solved with the molecular replacement method, with the MOLREP program of the CCP4 suite [25], and the structure of wild-type DTCS (Protein Data Bank [PDB] ID: 3GHM) as a starting model. After manual rebuilding with COOT [26], the model was refined with the REFMAC program in CCP4 [25] and CNS [27]. Data collection and refinement statistics are summarized in Table S1. Figures were generated with the PYMOL Molecular Graphics System (Version 1.5; Schrödinger, LLC, Boston, MA, USA). The atomic coordinates of DTCS-P475S have been deposited in the PDB (ID: 3VN4).

Expression and purification of MDTCS and MDTCS-P475S

Recombinant MDTCS and MDTCS-P475S (residues 75–685) were expressed in CHO Lec 3.2.8.1 cells [23] with a BelloCell Cell Culture System (CESCO Bioengineering, Taichung, Taiwan). After 50% (w/v) ammonium sulfate precipitation of the culture medium, MDTCS and MDTCS-P475S were each purified with an Ni^{2+}–NTA column followed by a Resource S cation-exchange column. Both recombinant proteins, when resolved on an SDS–polyacrylamide gel and stained with Coomassie Brilliant Blue, showed a single band of molecular mass 74 kDa, which coincided well with the molecular mass of 75 kDa estimated from their sequences. The protein concentration was determined by use of the 660-nm Protein Assay Reagent (Thermo Fisher Scientific, Waltham, MA, USA) with bovine serum albumin as a protein concentration standard, and adjusted to 1.8 nM in 10 mM Hepes (pH 7.4), 150 mM NaCl, 0.005% Tween-20, and 50% glycerol.

Kinetic analysis of FRETS-VWF73 cleavage by MDTCS and MDTCS-P475S

The kinetic parameters of MDTCS and MDTCS-P475S were determined with FRETS-VWF73 (Peptide Institute, Minoh, Japan), as described previously [28,29]. FRETS-VWF73 (0–4 μM) was incubated with 0.18 nM MDTCS or MDTCS-P475S in 10 mM Hepes (pH 7.4), 150 mM NaCl

and 0.005% Tween-20 at 37 °C. Fluorescence intensities were measured with the M × 3000p QPCR System (Agilent Technologies, Santa Clara, CA, USA) equipped with 340-nm excitation and 450-nm emission filters. The reaction rate was calculated by linear regression analysis of fluorescence over time from 0 to 60 min with PRISM 5 software (GraphPad Software, La Jolla, CA, USA). To obtain the reaction rate, various amounts of FRETS-VWF73 (5, 10, 20 and 50 μmol) were completely cleaved with 10 nM ADAMTS-13-MDTCS for 90 min, and their fluorescence intensities were used to estimate the amount of cleaved product (Fig. S1). The reaction rates as a function of substrate concentration were fitted to the Michaelis–Menten equation, and the maximum velocity (V_{max}), the rate constant (k_{cat}) and the affinity (K_m) were calculated with PRISM 5.

Cleavage of shear-treated VWF by MDTCS and MDTCS-P475S

The cleavage of shear-treated VWF by ADAMTS-13 was performed as described previously [30], with some modifications. Briefly, purified plasma VWF (25 μg mL^{-1}, 100 nM VWF monomers) [31] was vortexed at a rotation rate of 2500 r.p.m. for the indicated times in 10 mM Hepes (pH 7.4), 150 mM NaCl and 0.005% Tween-20 at 24 °C on a digital vortex mixer (Scientific Industries, Bohemia, NY, USA). MDTCS or MDTCS-P475S (1 nM each) was added to the VWF solution and incubated for the indicated times at 37 °C. The digested samples were separated by SDS-PAGE under reducing conditions, and transferred to a poly(vinylidene difluoride) membrane. The cleavage products were detected by western blotting with horseradish peroxidase-conjugated anti-VWF polyclonal antibody (Dako, Carpinteria, CA, USA) and the Luminata Forte Chemiluminescent Reagent (Millipore, Billerica, MA, USA). The band intensities of the cleavage products (150 kDa) were quantified with MULTI GAUGE software (Fuji Film, Tokyo, Japan).

Effects of denaturants and temperature on FRETS-VWF73 cleavage by MDTCS and MDTCS-P475S

MDTCS or MDTCS-P475S (1 nM each) was mixed with 1 μM FRETS-VWF73 in 10 mM Hepes (pH 7.4), 150 mM NaCl and 0.005% Tween-20 containing urea (0–2.5 M) or guanidine-HCl (0–0.5 M), and incubated for 2 min at 37 °C; the fluorescence intensities were then measured at 37 °C for 60 min. To investigate the effects of reaction temperature, the cleavage reaction mixtures were incubated for 2 min at 37, 40, 45 and 50 °C, and the fluorescence intensities were then measured for 60 min at the respective temperatures. The reaction rate was calculated by performing linear regression analysis of the plot of fluorescence against time from 0 to 60 min with PRISM 5.

Results

Crystal structure of DTCS-P475S

The overall structure of DTCS-P475S refined at 2.8-Å resolution is shown in Fig. 1A. The structure includes ADAMTS-13 residues 298–324, 328–458, and 466–682. The backbone structure of DTCS was very similar to the previously solved wild-type DTCS structure [18], with an overall root mean square deviation of 0.421 Å for 369 Cα atoms (Fig. 1B). The electron densities associated with the V-loop (Val474–Ala481) were clearly observed in the current DTCS-P475S structure (Fig. 1C), enabling a detailed structural comparison between the wild type and the mutant. The conformation of the V-loop in the C_A domain of DTCS-P475S was significantly different from that in two previously determined DTCS structures. In DTCS, an oxygen atom in the main chain of Pro475 formed hydrogen bonds with the side chains of Ser477 and Gln478, the distances of which were 3.5 Å/3.8 Å and 3.1 Å/3.5 Å, respectively (calculated from two DTCS structures) (PDB ID: 3GHM/3GHN) (Fig. 1D). On the other hand, these distances in DTCS-P475S were 5.0 Å and 8.3 Å, respectively (Fig. 1E). In the DTCS structure, Pro475 also formed van der Waals contacts with Met509 in the C_A domain (3.8 Å/3.5 Å) and with Leu620 in the β6–β7 loop of the S domain (3.5 Å/4.0 Å), and stabilized the structure (Fig. 1D). The distances between Ser475 and Met509 (7.1 Å), and between Ser475 and Leu620 (5.1Å), were longer in DTCS-P475S than in DTCS, where the interactions no longer occurred (Fig. 1E). The lack of obvious interactions of Ser475 with other residues in the C_A and S domains in DTCS-P475S suggests that the V-loop structure is less stable in DTCS-P475S than in DTCS. The structures of the other loops in the C_A domain of DTCS-P475S did not differ significantly from those of DTCS.

Electron densities for the carbohydrate moieties of two potential *N*-linked sites (Asn552 and Asn614) and a potential *O*-linked site (Ser399) were present in both DTCS-P475S and DTCS [18]. An electron density linked to the side chain of Trp387 in the T1 domain was detected in DTCS-P475S (Fig. 1F). Trp387 is a conserved *C*-mannosylation site (WXXW, where the first tryptophan would be glycosylated), and *C*-mannosylation has been observed on conserved tryptophan residues in a number of TSRs [32], including ADAMTS-5 [33], suggesting that Trp387 is possibly *C*-mannosylated, although this modification was not clear in the electron densities of wild-type DTCS structures. In *C*-mannosylation, a mannose group is added to the C2 atom of the tryptophan.

Kinetic parameters of MDTCS and MDTCS-P475S

We measured the ADAMTS-13 activities of MDTCS and MDTCS-P475S with FRETS-VWF73, and determined their kinetic parameters. The cleavage reaction was monitored as

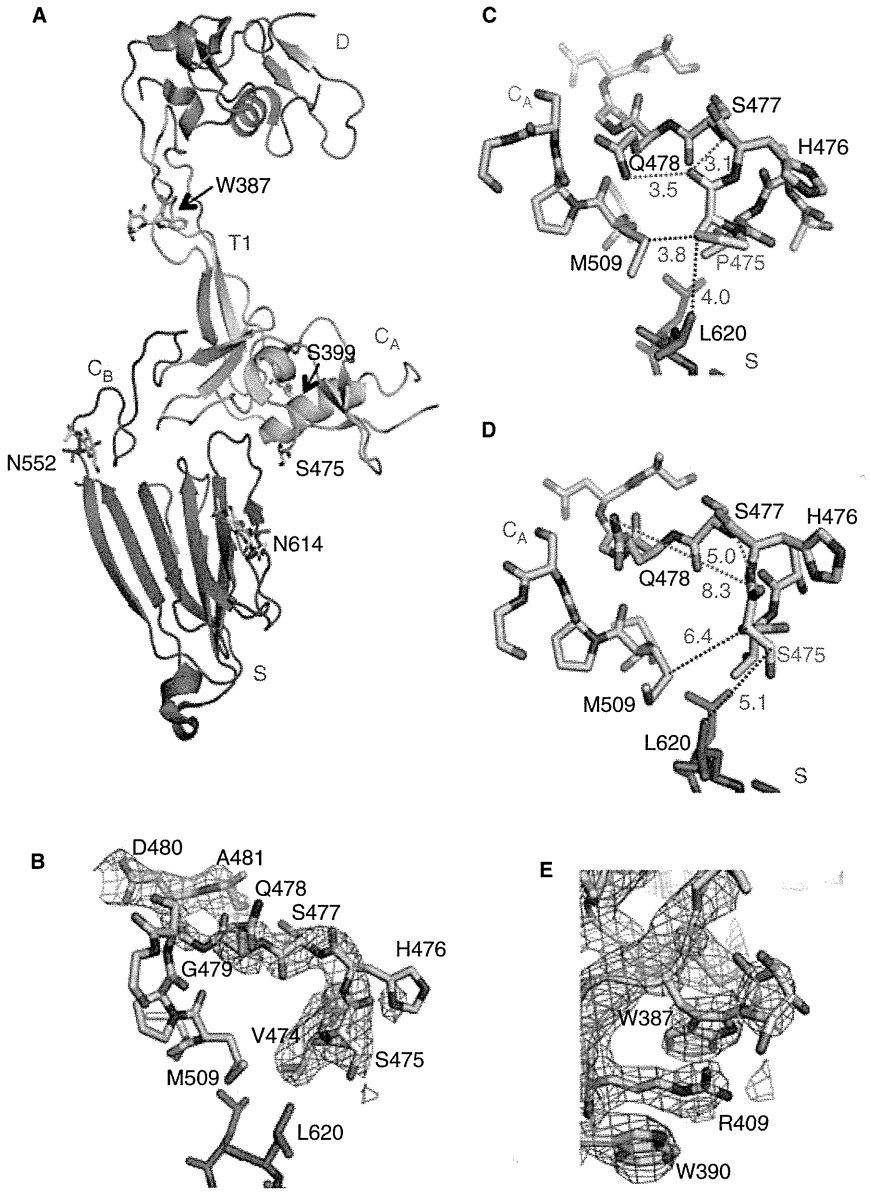

Fig. 1. Crystal structure of DTCS-P475S. (A) Overall structure of DTCS-P475S. Potential *N*-glycosylation at Asn552 (in the C_B domain) and Asn614 (in the S domain), *O*-fucosylation at Ser399 (in the T1 domain), and *C*-mannosylation at Trp387 (in the T1 domain) are shown as stick models. D, orange; T1, cyan; C_A, green; C_B, red; S, magenta. (B) A $2F_o - F_c$ electron density map (contoured at 1.2σ) associated with the V-loop in the C_A domain of DTCS-P475S. (C, D) Close-up view around the V-loop of the C_A domain in DTCS (C) and DTCS-P475S (D). The magenta and blue dotted lines show the hydrogen bonds and van der Waals contacts, respectively, of Pro475 in DTCS (C, PDB ID: 3GHN). For comparison, the corresponding lines are also shown in DTCS-P475S (D). The blue numbers show the distances between the atoms (Å). (E) A $2F_o - F_c$ electron density map (contoured at 1.2σ) is associated with the carbohydrate moiety linked to Trp387, most likely mannose.

an increase in the fluorescence of cleaved FRETS-VWF73, and converted to the reaction rate. The reaction showed typical Michaelis–Menten kinetics (Fig. 2). The V_{max} values of MDTCS and MDTCS-P475S were the same (0.35 nM s^{-1}), and their k_{cat} values were similar (MDTCS, 1.94 ± 0.08 s^{-1}; MDTCS-P475S, 1.90 ± 0.11 s^{-1}; Table 1). On the other hand, the K_m of MDTCS-P475S (0.82 ± 0.12 μM) was two-fold higher than that of MDTCS (0.37 ± 0.06 μM). These results indicated that the P475S substitution in MDTCS resulted in a two-fold reduction in catalytic efficiency (k_{cat}/K_m), mainly because of its lower affinity for FRETS-VWF73. We performed a thermal shift assay involving MDTCS and MDTCS-P475S by using SYPRO Orange (Fig. S2). The T_m values of MDTCS and MDTCS-P475S were identical in the absence (50 °C) and presence (46 °C) of 1.5 M urea.

Shear-treated VWF cleavage by MDTCS and MDTCS-P475S

As the scissile Tyr1605–Met1606 bond of VWF is buried within the core of the globular A2 domain [34], VWF under static conditions is not a good substrate for ADAMTS-13.

Table 1 Michaelis–Menten kinetic parameters of MDTCS and MDTCS-P475S

	MDTCS	MDTCS-P475S
K_m (μM)	0.37 ± 0.06	0.82 ± 0.12
k_{cat} (s^{-1})	1.94 ± 0.08	1.90 ± 0.11
k_{cat}/K_m (μM^{-1} s^{-1})	5.26 ± 0.52	2.32 ± 0.67
V_{max} (nM s^{-1})	0.35 ± 0.02	0.35 ± 0.02

Values are means ± standard deviation.

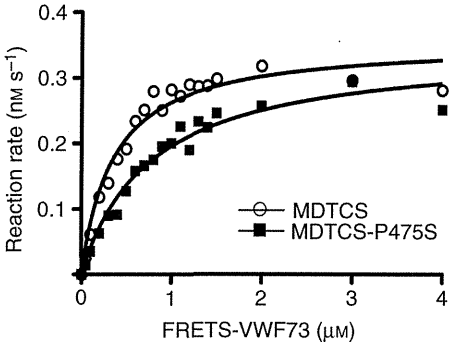

Fig. 2. Kinetic analysis of the cleavage of FRETS-VWF73 by MDTCS and MDTCS-P475S. FRETS-VWF73 (0.05–4 μM) was incubated with MDTCS (open circles, 0.18 nM) or MDTCS-P475S (closed squares, 0.18 nM) at 37 °C. The reaction rate was obtained from the increase in fluorescence over time. The line represents the non-linear fit to the Michaelis–Menten equation. VWF, von Willebrand factor.

When VWF is subjected to shear stress in circulation in vivo or denaturants in vitro, the A2 domain unfolds and adopts a partially extended conformation that makes its scissile peptide bond accessible for cleavage by ADAMTS-13 [19,35]. VWF treated with mechanistic-induced flow on a vortex mixer can be easily cleaved by ADAMTS-13 [30], so this fluid shear-treated VWF-cleaving assay is useful for the investigation of ADAMTS-13 function and regulation. We examined the activities of MDTCS and MDTCS-P475S against shear-treated VWF. VWF cleavage was monitored by the appearance of the 150-kDa band on western blotting with the anti-VWF antibody. Although both MDTCS and MDTCS-P475S produced the 150-kDa fragment band after a 10-min incubation, the band intensity was weaker for MDTCS-P475S (63% ± 8.2% at 120 min) than for MDTCS (Fig. 3A). Shearing treatment of MDTCS-P475S did not affect VWF-cleaving activity (Fig. 3B). These results suggest that MDTCS-P475S moderately cleaves VWF, once the scissile bond in VWF is exposed by shear stress. Shear treatment-induced cleavage of VWF by MDTCS-P475S was more severely inhibited than that by MDTCS upon the addition of urea. The VWF-cleaving activities of MDTCS and MDTCS-P475S in the presence of 1.5 M urea were 47.0% ± 6.5% and 8.9% ± 1.9%, respectively (Fig. 3C).

Effects of denaturants and temperature on the enzymatic activities of MDTCS and MDTCS-P475S

As the addition of urea severely inhibited the shear-dependent cleavage of VWF by MDTCS-P475S, we examined the effects of denaturants on the activity of MDTCS and MDTCS-P475S by using FRETS-VWF73. The reaction rates of MDTCS and MDTCS-P475S were

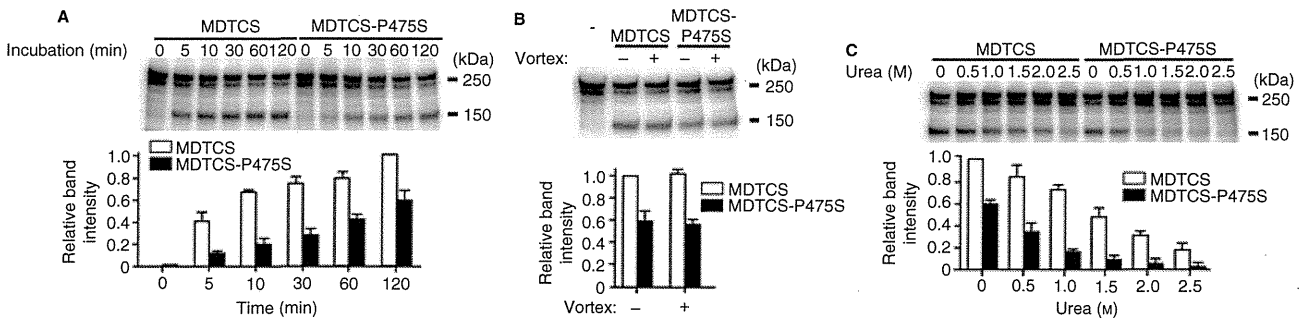

Fig. 3. Cleavage of shear-treated von Willebrand factor (VWF) by MDTCS and MDTCS-P475S. (A) Top: western blotting image showing VWF cleavage at each time point. The VWF multimer (25 μg mL^{-1}; 100 nM VWF monomers) was treated with shear with a 3-min vortex at 2500 r.p.m. at 24 °C, and MDTCS or MDTCS-P475S (1 nM) was then added to the reaction mixture. After incubation for the indicated times (0–120 min) at 37 °C, VWF cleavage was detected by the appearance of the 150-kDa band on western blotting with the anti-VWF antibody. Bottom: densitometric analysis of VWF cleavage. The band intensities of the cleavage products (150 kDa) were quantified as described in Materials and Methods. Band intensities relative to that of MDTCS at 120 min (set as 1) were plotted as means ± standard deviation (n = 3). (B) Top: western blotting image showing VWF cleavage by shear-treated or untreated MDTCS or MDTCS-P475S. The VWF multimer (25 μg mL^{-1}) was treated by shearing with vortexing for 3 min, and MDTCS or MDTCS-P475S (1 nM each), treated with shearing (2500 r.p.m. for 10 min), was then added to the reaction mixture. After incubation for 120 min at 37 °C, the cleavage of shear-treated VWF was detected as described in (A). Bottom: densitometric analysis of VWF cleavage. Band intensities relative to that of MDTCS without vortex (set as 1) were plotted as means ± standard deviation (n = 3). (C) Top: western blotting image showing VWF cleavage at various concentrations of urea. The VWF multimer (25 μg mL^{-1}) was treated with shear with a 3-min vortex, and MDTCS or MDTCS-P475S (1 nM each) was then added to the reaction mixture containing 0–2.5 M urea. After incubation for 120 min at 37 °C, the cleavage of shear-treated VWF was detected as described in (A). Bottom: densitometric analysis of VWF cleavage. Band intensities relative to that of MDTCS at 0 M urea (set as 1) were plotted as means ± standard deviation (n = 3).

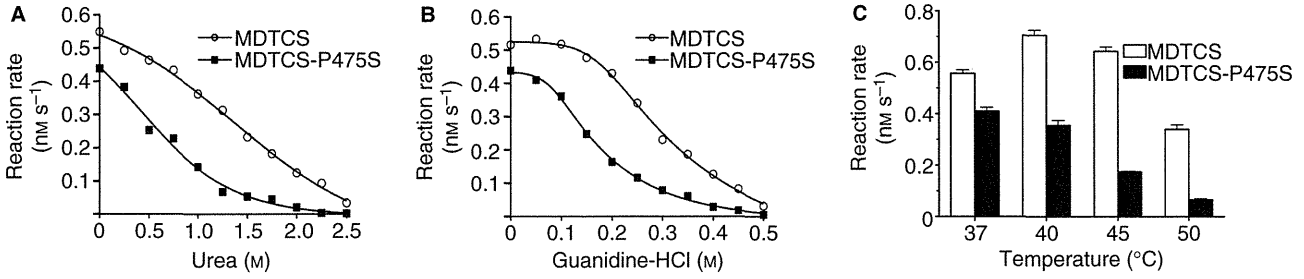

Fig. 4. Effects of denaturants and temperature on the FRETS-VWF73-cleaving activity of MDTCS and MDTCS-P475S. The enzymatic activities of MDTCS and MDTCS-P475S (0.8 nM) were measured for 60 min by the use of FRETS-VWF73 (1 μM) in the presence of urea (A) or guanidine-HCl (B) at 37 °C, or at different reaction temperatures (C). Values are means ± standard deviation (C: n = 3). VWF, von Willebrand factor.

reduced according to the concentrations of urea (Fig. 4A) or guanidine-HCl (Fig. 4B). The half-maximal inhibitory concentration (IC_{50}) for urea was 1.5 M for MDTCS and 0.8 M for MDTCS-P475S. The IC_{50} for guanidine-HCl was 0.3 M for MDTCS and 0.15 M for MDTCS-P475S. Furthermore, the activities of MDTCS and MDTCS-P475S were measured at 37, 40, 45 and 50 °C (Fig. 4C). A higher reaction temperature caused a more severe decrease in the activity of MDTCS-P475S than of MDTCS.

Discussion

Racial or ethnic group-specific genetic factors are now recognized to be important factors in the pathogenesis of thrombosis [36,37]. We previously identified the dysfunctional P475S polymorphism in ADAMTS-13 [8], and showed that it is East Asian-specific [14]. In the present study, we demonstrated that MDTCS-P475S showed moderate cleavage activity against shear-treated VWF, suggesting that the P475S polymorphism is not a causative factor in the development of TTP. However, this does not exclude the possibility that the P475S polymorphism could increase the risk for acquired TTP caused by inhibitory autoantibodies against ADAMTS-13. The relationship of the P475S polymorphism with acquired TTP remains to be addressed.

Recent studies have indicated the important function of the D and S domains as substrate-binding exosites [19–21]. We have identified at least three putative VWF-binding exosites, within the D, C_A and S domains, linearly aligned in the three-dimensional structure [18]. In the present study, kinetic analysis with FRETS-VWF73 showed that the lower catalytic efficiency (k_{cat}/K_m) of MDTCS-P475S was caused by lower affinity (higher K_m) but not by lower catalytic activity (lower k_{cat}). This also supports the idea that the V-loop in the C_A domain is a VWF-binding exosite.

The thermal shift assay showed that the thermostabilities of MDTCS and MDTCS-P475S were almost the same. Although the interaction between Ser475 in the V-loop of the C_A domain and Leu620 in the β6–β7 loop of the S domain was disrupted in the MDTCS-P475S structure, van der Waals contacts between Leu621 in the S domain and a hydrophobic pocket in the C_A domain formed by Gln442, Leu443, Met446, Val474, Arg507, Cys508 and Met509 [18] were retained. These interactions may minimize the adverse effect of P475S substitution on the stability of the S domain. These observations suggest that the reduction in the activity of MDTCS-P475S is not a consequence of global protein instability, but rather of a reduction in the enzyme–substrate interaction owing to the local conformational change in the V-loop (especially interatomic interactions with Ser475) (Fig. 1D). The greatly reduced enzymatic activity of MDTCS-P475S in the presence of urea and at a higher reaction temperature suggests that the P475S substitution induces a more severe local conformational change in the V-loop under these conditions and reduces the enzyme–substrate interaction.

Pro475 is conserved in all primates examined but not in other species (Fig. S3). Mouse ADAMTS-13 shows significantly reduced enzymatic activity against human VWF [38], indicating the species specificity of the ADAMTS-13–VWF interaction. Several amino acids in the core binding region for ADAMTS-13 in the A2 domain of VWF (VWF73) [39] differ among species (Fig. S4). Non-conserved amino acids in the exosites of ADAMTS-13 and in the VWF73 region of VWF may have coevolved for species-specific ADAMTS-13–VWF interface recognition.

Post-translational protein *C*-mannosylation is the attachment of an α-mannopyranosyl residue to the indole C-2 of tryptophan via a C–C linkage [32]. Proteins known to be *C*-mannosylated are RNase, interleukin-12, the mucins MUC5AC and MUC5B, and several proteins containing TSRs, such as thrombospondin-1, F-spondin, C6, C7, properdin, ADAMTS-L1, and ADAMTS-5 [33]. In the present study, potential *C*-mannosylation of Trp387 in the T1 domain of ADAMTS-13 has been suggested for the first time. *C*-mannosylation typically occurs in TSRs within the sequence motif W*XX*W, which is highly conserved among ADAMTS family members (ADAMTSs and ADAMTS-Ls) [33]. The functional role of *C*-mannosylation in ADAMTS-13 is unknown; however, a *C*-

mannosylation defect in ADAMTS-L1 decreases its secretion, suggesting a role in the regulation of protein secretion [33].

Addendum

M. Akiyama, D. Nakayama, and S. Takeda: performed research, analyzed data, and wrote the manuscript; K. Kokame: designed the experiments; J. Takagi: provided laboratory reagents; T. Miyata: wrote the manuscript and provided funding. All authors have approved the final draft.

Acknowledgements

The authors thank Y. Fujimura at Nara Medical University for providing us with purified plasma VWF. We also thank T. Kunieda for her help with protein purification, and M. Tomisako for her help with crystallization. This work was supported by grants-in-aid from the Ministry of Health, Labor, Welfare of Japan, the Ministry of Education, Culture, Sports, Science and Technology of Japan, and the SENSHIN Medical Research Foundation.

Disclosure of Conflict of Interests

The authors state that they have no conflict of interest.

Supporting Information

Additional Supporting Information may be found in the online version of this article:

Figure S1. Calibration curves for FRETS-VWF73 cleavage.
Figure S2. Thermal shift assay profiles of MDTCS and MDTCS-P475S.
Figure S3. Amino acid sequence alignment of the C_A domain of ADAMTS-13 from different species.
Figure S4. Amino acid sequence alignment of the core binding region for ADAMTS-13 in the A2 domain of VWF from different species.
Table S1. Data collection and refinement statistics.

References

1 Springer TA. Biology and physics of von Willebrand factor concatamers. *J Thromb Haemost* 2011; **9**(Suppl. 1): 130–43.
2 Dent JA, Galbusera M, Ruggeri ZM. Heterogeneity of plasma von Willebrand factor multimers resulting from proteolysis of the constituent subunit. *J Clin Invest* 1991; **88**: 774–82.
3 Tsai HM, Sussman II, Nagel RL. Shear stress enhances the proteolysis of von Willebrand factor in normal plasma. *Blood* 1994; **83**: 2171–9.
4 Sadler JE, Moake JL, Miyata T, George JN. Recent advances in thrombotic thrombocytopenic purpura. *Hematology Am Soc Hematol Educ Program* 2004; **2004**: 407–23.
5 Soejima K, Mimura N, Hirashima M, Maeda H, Hamamoto T, Nakagaki T, Nozaki C. A novel human metalloprotease synthesized in the liver and secreted into the blood: possibly, the von Willebrand factor-cleaving protease? *J Biochem* 2001; **130**: 475–80.
6 Levy GG, Nichols WC, Lian EC, Foroud T, McClintick JN, McGee BM, Yang AY, Siemieniak DR, Stark KR, Gruppo R, Sarode R, Shurin SB, Chandrasekaran V, Stabler SP, Sabio H, Bouhassira EE, Upshaw JD Jr, Ginsburg D, Tsai HM. Mutations in a member of the ADAMTS gene family cause thrombotic thrombocytopenic purpura. *Nature* 2001; **413**: 488–94.
7 Zheng X, Chung D, Takayama TK, Majerus EM, Sadler JE, Fujikawa K. Structure of von Willebrand factor-cleaving protease (ADAMTS13), a metalloprotease involved in thrombotic thrombocytopenic purpura. *J Biol Chem* 2001; **276**: 41059–63.
8 Kokame K, Matsumoto M, Soejima K, Yagi H, Ishizashi H, Funato M, Tamai H, Konno M, Kamide K, Kawano Y, Miyata T, Fujimura Y. Mutations and common polymorphisms in ADAMTS13 gene responsible for von Willebrand factor-cleaving protease activity. *Proc Natl Acad Sci USA* 2002; **99**: 11902–7.
9 Lotta LA, Garagiola I, Palla R, Cairo A, Peyvandi F. ADAMTS13 mutations and polymorphisms in congenital thrombotic thrombocytopenic purpura. *Hum Mutat* 2010; **31**: 11–19.
10 Kokame K, Kokubo Y, Miyata T. Polymorphisms and mutations of ADAMTS13 in the Japanese population and estimation of the number of patients with Upshaw–Schulman syndrome. *J Thromb Haemost* 2011; **9**: 1654–6.
11 Jang MJ, Kim NK, Chong SY, Kim HJ, Lee SJ, Kang MS, Oh D. Frequency of Pro475Ser polymorphism of ADAMTS13 gene and its association with ADAMTS-13 activity in the Korean population. *Yonsei Med J* 2008; **49**: 405–8.
12 Gao W, Ruan C, Dai L, Su J, Wang Z. The frequency of P475S polymorphism in von Willebrand factor-cleaving protease in the Chinese population and its relevance to arterial thrombotic disorders. *Thromb Haemost* 2004; **91**: 1257–8.
13 Bongers TN, De Maat MP, Dippel DW, Uitterlinden AG, Leebeek FW. Absence of Pro475Ser polymorphism in ADAMTS-13 in Caucasians. *J Thromb Haemost* 2005; **3**: 805.
14 Kokame K, Miyata T. Genetic defects leading to hereditary thrombotic thrombocytopenic purpura. *Semin Hematol* 2004; **41**: 34–40.
15 Akiyama M, Kokame K, Miyata T. ADAMTS13 P475S polymorphism causes a lowered enzymatic activity and urea lability *in vitro*. *J Thromb Haemost* 2008; **6**: 1830–2.
16 Soejima K, Matsumoto M, Kokame K, Yagi H, Ishizashi H, Maeda H, Nozaki C, Miyata T, Fujimura Y, Nakagaki T. ADAMTS-13 cysteine-rich/spacer domains are functionally essential for von Willebrand factor cleavage. *Blood* 2003; **102**: 3232–7.
17 Zheng X, Nishio K, Majerus EM, Sadler JE. Cleavage of von Willebrand factor requires the spacer domain of the metalloprotease ADAMTS13. *J Biol Chem* 2003; **278**: 30136–41.
18 Akiyama M, Takeda S, Kokame K, Takagi J, Miyata T. Crystal structures of the noncatalytic domains of ADAMTS13 reveal multiple discontinuous exosites for von Willebrand factor. *Proc Natl Acad Sci USA* 2009; **106**: 19274–9.
19 Crawley JT, de Groot R, Xiang Y, Luken BM, Lane DA. Unraveling the scissile bond: how ADAMTS13 recognizes and cleaves von Willebrand factor. *Blood* 2011; **118**: 3212–21.
20 Wu JJ, Fujikawa K, McMullen BA, Chung DW. Characterization of a core binding site for ADAMTS-13 in the A2 domain of von Willebrand factor. *Proc Natl Acad Sci USA* 2006; **103**: 18470–4.
21 Jin SY, Skipwith CG, Zheng XL. Amino acid residues Arg(659), Arg(660), and Tyr(661) in the spacer domain of ADAMTS13 are critical for cleavage of von Willebrand factor. *Blood* 2010; **115**: 2300–10.

22 Pos W, Crawley JT, Fijnheer R, Voorberg J, Lane DA, Luken BM. An autoantibody epitope comprising residues R660, Y661, and Y665 in the ADAMTS13 spacer domain identifies a binding site for the A2 domain of VWF. *Blood* 2010; **115**: 1640–9.
23 Akiyama M, Takeda S, Kokame K, Takagi J, Miyata T. Production, crystallization and preliminary crystallographic analysis of an exosite-containing fragment of human von Willebrand factor-cleaving proteinase ADAMTS13. *Acta Crystallogr F Struct Biol Crystallogr Commun* 2009; **65**: 739–42.
24 Reeves PJ, Callewaert N, Contreras R, Khorana HG. Structure and function in rhodopsin: high-level expression of rhodopsin with restricted and homogeneous *N*-glycosylation by a tetracycline-inducible *N*-acetylglucosaminyltransferase I-negative HEK293S stable mammalian cell line. *Proc Natl Acad Sci USA* 2002; **99**: 13419–24.
25 Winn MD, Ballard CC, Cowtan KD, Dodson EJ, Emsley P, Evans PR, Keegan RM, Krissinel EB, Leslie AG, McCoy A, McNicholas SJ, Murshudov GN, Pannu NS, Potterton EA, Powell HR, Read RJ, Vagin A, Wilson KS. Overview of the CCP4 suite and current developments. *Acta Crystallogr D Biol Crystallogr* 2011; **67**: 235–42.
26 Emsley P, Lohkamp B, Scott WG, Cowtan K. Features and development of Coot. *Acta Crystallogr D Biol Crystallogr* 2010; **66**: 486–501.
27 Brunger AT. Version 1.2 of the crystallography and NMR system. *Nat Protoc* 2007; **2**: 2728–33.
28 Kokame K, Nobe Y, Kokubo Y, Okayama A, Miyata T. FRETS-VWF73, a first fluorogenic substrate for ADAMTS13 assay. *Br J Haematol* 2005; **129**: 93–100.
29 Anderson PJ, Kokame K, Sadler JE. Zinc and calcium ions cooperatively modulate ADAMTS13 activity. *J Biol Chem* 2006; **281**: 850–7.
30 Zhang P, Pan W, Rux AH, Sachais BS, Zheng XL. The cooperative activity between the carboxyl-terminal TSP1 repeats and the CUB domains of ADAMTS13 is crucial for recognition of von Willebrand factor under flow. *Blood* 2007; **110**: 1887–94.
31 De Marco L, Shapiro SS. Properties of human asialo-factor VIII. A ristocetin-independent platelet-aggregating agent. *J Clin Invest* 1981; **68**: 321–8.
32 Gonzalez de Peredo A, Klein D, Macek B, Hess D, Peter-Katalinic J, Hofsteenge J. *C*-mannosylation and *O*-fucosylation of thrombospondin type 1 repeats. *Mol Cell Proteomics* 2002; **1**: 11–18.
33 Wang LW, Leonhard-Melief C, Haltiwanger RS, Apte SS. Post-translational modification of thrombospondin type-1 repeats in ADAMTS-like 1/punctin-1 by *C*-mannosylation of tryptophan. *J Biol Chem* 2009; **284**: 30004–15.
34 Zhang Q, Zhou YF, Zhang CZ, Zhang X, Lu C, Springer TA. Structural specializations of A2, a force-sensing domain in the ultralarge vascular protein von Willebrand factor. *Proc Natl Acad Sci USA* 2009; **106**: 9226–31.
35 Zhang X, Halvorsen K, Zhang CZ, Wong WP, Springer TA. Mechanoenzymatic cleavage of the ultralarge vascular protein von Willebrand factor. *Science* 2009; **324**: 1330–4.
36 Zakai NA, McClure LA. Racial differences in venous thromboembolism. *J Thromb Haemost* 2011; **9**: 1877–82.
37 Miyata T, Hamasaki N, Wada H, Kojima T. More on: racial differences in venous thromboembolism. *J Thromb Haemost* 2012; **10**: 319–20.
38 Zhou W, Bouhassira EE, Tsai HM. An IAP retrotransposon in the mouse ADAMTS13 gene creates ADAMTS13 variant proteins that are less effective in cleaving von Willebrand factor multimers. *Blood* 2007; **110**: 886–93.
39 Kokame K, Matsumoto M, Fujimura Y, Miyata T. VWF73, a region from D1596 to R1668 of von Willebrand factor, provides a minimal substrate for ADAMTS-13. *Blood* 2004; **103**: 607–12.

Thrombosis Research 132 (2013) 314–315

Contents lists available at ScienceDirect

Thrombosis Research

journal homepage: www.elsevier.com/locate/thromres

Letter to the Editors-in-Chief

Protein S K196E mutation, a genetic risk factor for venous thromboembolism, is limited to Japanese

Dear Editors,

Ethnic differences in thrombotic genetic risk have received much attention in recent years because the established thrombotic genetic variants, factor V Leiden and prothrombin G20210A mutation, are limited in Caucasian populations but not in East Asian populations [1]. We and others have identified the protein S K196E mutation (rs121918474) as a genetic risk factor for venous thromboembolism (VTE) in a Japanese population with odds ratios between 3.74 and 8.56 [2–5]. The allele frequency of this mutation is 0.0089 [5,6]. When overlapping with congenital protein C deficiency, this mutation facilitates the development of VTE [4,7]. The individuals heterozygous for the mutant E-allele had 16% lower protein S anticoagulant activity than wild-type subjects [8]. An *in vitro* study showed that the recombinant protein S with the K196E mutation lost activated protein C-dependent anticoagulant activity [9]. Since East Asians including Japanese, Chinese, and Koreans are geographically and genetically close, the protein S K196E mutation, which has so far been found only in Japanese, may be found in other East Asians. In this study, we have genotyped the protein S K196E mutation in Chinese and Korean populations to clarify the geographic distribution of this thrombotic mutation. The mutation was not found in Chinese or Koreans.

The first panel for the genotyping was a general Chinese population consisting of 509 individuals: 50 in Dehui, 49 in Huludao, 50 in Beijing, 49 in Jinan, 50 in Xi'an, 47 in Baoji, 50 in Shanghai, 50 in Changsha, 15 in Heping, 50 in Nanning, and 49 in Tainan. The second panel was a general Korean population consisting of 492 individuals including 105 in Seoul, 29 in Chonan, 46 in Haman, 247 in Pusan, and 65 in Jeju-do [10,11]. The third panel consisted of 122 Chinese patients with VTE and 112 Chinese control individuals [12]. Furthermore, from the 1000 Genomes Project (http://www.1000genomes.org/) we retrieved the genetic information of protein S K196E mutation in 197 Chinese consisting of 97 Chinese in Beijing and 100 Chinese in southern China, as well as in 89 Japanese [13].

The genotype of protein S K196E mutation in the first two panels was determined by the TaqMan genotype discrimination method [8] using the primers 5'- ACCACTGTTCCTGTAAAAATGGTTT/5'- TTTAATT CTACCATCCTGCTCTTACCT and the probes 5'-FAM - CAATCTTTCTtAT TTGAAAGC-MGB (the wild-type allele)/5'-VIC- AATCTTTCTcATTTGA AAGC (the mutant allele). In the third panel, we genotyped the mutation by the Homogeneous Mass Extend and iPLEX assays (Sequenom, Hamburg, Germany) and validated it with the SNaPshot assay (Applied Biosystems, USA). Primer sequences of the SEQUENOM assay are available on request. The PCR primers for the SNaPshot were AGACATAA ATGAACGCAAAGATC and TCTAACTGGGATTATTCTCACAC, and the sequence for the extension probe was TTTTTTTTTTTTTTCTTACCTTTACA GTCTTTCT. The SNaPshot products were resolved and analyzed using an ABI 3730 Automated Sequence Analyzer (Applied Biosystems). The study protocol was approved by the Institutional Review Boards and Ethics Committees of Kyoto University School of Medicine and by the General Hospital of the People's Liberation Army.

We genotyped the protein S K196E mutation in 509 Chinese and 492 Koreans and found that none carried the mutation. We did not identify the mutation in 122 Chinese patients with VTE or in 112 Chinese control individuals. Thus, the genetic analysis of three independent panels indicated that the protein S K196E mutation is present solely in Japanese and not in Chinese. The number of Korean individuals we genotyped was insufficient to yield conclusive evidence, and the 1000 Genomes Project does not include Koreans, but it is likely that Koreans also do not carry the mutation. The 1000 Genomes Project showed that none of the 197 Chinese carried the protein S K196E mutation, but one heterozygous carrier was present in 89 Japanese. We calculated a statistical power to detect a difference of minor allele frequency between Japanese and Chinese/Korean with the 0.05 level of significance. A one-sided statistical power more than 0.80 was considered statistically significant. Albeit a large enough statistical power for Chinese (0.82), a low statistical power, 0.67, for Korean may permit us to apply above argument to only Chinese.

The finding that the protein S K196E mutation is present only in Japanese was unexpected, because in thrombosis-related factors, two genetic mutations found in Japanese but not in Caucasians, plasminogen A620T and ADAMTS13 P475S, are both present in Chinese and Koreans [14,15]. The present results suggest that, even though Japanese, Chinese, and Koreans are geographically close to one another, the genetic background for thrombosis differs among them. The results also suggest that the protein S K196E mutation is a recent occurrence and fixed within the Japanese population.

Conflict of Interest Statement

The authors state that they have no conflict of interest.

Acknowledgments

We thank Dr. Hiroko Shirotani-Ikejima for her excellent technical assistance. This work was supported in part by grants-in-aid from the Ministry of Health, Labour, and Welfare of Japan; the Ministry of Education, Culture, Sports, Science, and Technology of Japan; the Japan Society for the Promotion of Science; and by the National Natural Science Foundation of China (No. 30971259). The research activity of X. P. Fan, of the Beijing Chaoyang Hospital affiliated with the Capital Medical University of China, was supported by a Scholarship from the Takeda Foundation.

References

[1] Zakai NA, McClure LA. Racial differences in venous thromboembolism. J Thromb Haemost 2011;9:1877–82.
[2] Kinoshita S, Iida H, Inoue S, Watanabe K, Kurihara M, Wada Y. Protein S and protein C gene mutations in Japanese deep vein thrombosis patients. Clin Biochem 2005;38:908–15.

0049-3848/$ – see front matter
http://dx.doi.org/10.1016/j.thromres.2013.05.008

[3] Kimura R, Honda S, Kawasaki T, Tsuji H, Madoiwa S, Sakata Y, et al. Protein S-K196E mutation as a genetic risk factor for deep vein thrombosis in Japanese patients. Blood 2006;107:1737–8.
[4] Ikejiri M, Wada H, Sakamoto Y, Ito N, Nishioka J, Nakatani K, et al. The association of protein S Tokushima-K196E with a risk of deep vein thrombosis. Int J Hematol 2010;92:302–5.
[5] Miyata T, Kimura R, Kokubo Y, Sakata T. Genetic risk factors for deep vein thrombosis among Japanese: importance of protein S K196E mutation. Int J Hematol 2006;83: 217–23.
[6] Miyata T, Hamasaki N, Wada H, Kojima T. More on: racial differences in venous thromboembolism. J Thromb Haemost 2012;10:319–20.
[7] Miyata T, Sato Y, Ishikawa J, Okada H, Takeshita S, Sakata T, et al. Prevalence of genetic mutations in protein S, protein C and antithrombin genes in Japanese patients with deep vein thrombosis. Thromb Res 2009;124:14–8.
[8] Kimura R, Sakata T, Kokubo Y, Okamoto A, Okayama A, Tomoike H, et al. Plasma protein S activity correlates with protein S genotype but is not sensitive to identify K196E mutant carriers. J Thromb Haemost 2006;4:2010–3.
[9] Hayashi T, Nishioka J, Suzuki K. Molecular mechanism of the dysfunction of protein S(Tokushima) (Lys155– > Glu) for the regulation of the blood coagulation system. Biochim Biophys Acta 1995;1272:159–67.
[10] Liu W, Morito D, Takashima S, Mineharu Y, Kobayashi H, Hitomi T, et al. Identification of RNF213 as a susceptibility gene for moyamoya disease and its possible role in vascular development. PLoS One 2011;6:e22542.
[11] Liu W, Hitomi T, Kobayashi H, Harada KH, Koizumi A. Distribution of moyamoya disease susceptibility polymorphism p.R4810K in RNF213 in East and Southeast Asian Populations. Neurol Med Chir (Tokyo) 2012;52:299–303.
[12] Xu Q, Xu B, Zhang Y, Yang J, Gao L, Wang H, et al. Estimation of the warfarin dose with a pharmacogenetic refinement algorithm in Chinese patients mainly under low-intensity warfarin anticoagulation. Thromb Haemost 2012;108:1132–40.
[13] Abecasis GR, Auton A, Brooks LD, DePristo MA, Durbin RM, Handsaker RE, et al. An integrated map of genetic variation from 1,092 human genomes. Nature 2012;491:56–65.
[14] Ooe A, Kida M, Yamazaki T, Park SC, Hamaguchi H, Girolami A, et al. Common mutation of plasminogen detected in three Asian populations by an amplification refractory mutation system and rapid automated capillary electrophoresis. Thromb Haemost 1999;82:1342–6.
[15] Ruan C, Dai L, Su J, Wang Z. The frequency of P475S polymorphism in von Willebrand factor-cleaving protease in the Chinese population and its relevance to arterial thrombotic disorders. Thromb Haemost 2004;91:1257–8.

Wanyang Liu
Department of Health and Environmental Sciences, Kyoto University Graduate School of Medicine, Kyoto, Japan
Department of Occupational and Environmental Health, School of Public Health, China Medical University, Shenyang, China

Tong Yin
Yang Li
Bin Xu
Jie Yang
Hongjuan Wang
Institute of Geriatric Cardiology, General Hospital of Chinese People's Liberation Army, Beijing, China

Hiroko Okuda
Kouji H. Harada
Akio Koizumi
Department of Health and Environmental Sciences, Kyoto University Graduate School of Medicine, Kyoto, Japan

Xinping Fan
Department of Molecular Pathogenesis, National Cerebral and Cardiovascular Center, Suita, Osaka, Japan
Department of Clinical Laboratory, Beijing Chaoyang Hospital, Capital Medical University, Beijing, China

Toshiyuki Miyata
Department of Molecular Pathogenesis, National Cerebral and Cardiovascular Center, Suita, Osaka, Japan
Corresponding author. Tel.: +81 6 6833 5012; fax: +81 6 6835 1176.
E-mail address: miyata@ri.ncvc.go.jp.

27 March 2013

The Integrin-Linked Kinase-PINCH-Parvin Complex Supports Integrin αIIbβ3 Activation

Shigenori Honda[1*], Hiroko Shirotani-Ikejima[1], Seiji Tadokoro[2], Yoshiaki Tomiyama[2,3], Toshiyuki Miyata[1]

1 Department of Molecular Pathogenesis, National Cerebral and Cardiovascular Center, Suita, Japan, **2** Department of Hematology and Oncology, Osaka University Graduate School of Medicine, Suita, Osaka, Japan, **3** Department of Blood Transfusion, Osaka University Hospital, Suita, Osaka, Japan

Abstract

Integrin-linked kinase (ILK) is an important signaling regulator that assembles into the heteroternary complex with adaptor proteins PINCH and parvin (termed the IPP complex). We recently reported that ILK is important for integrin activation in a Chinese hamster ovary (CHO) cell system. We previously established parental CHO cells expressing a constitutively active chimeric integrin (αIIbα6Bβ3) and mutant CHO cells expressing inactive αIIbα6Bβ3 due to ILK deficiency. In this study, we further investigated the underlying mechanisms for ILK-dependent integrin activation. ILK-deficient mutant cells had trace levels of PINCH and α-parvin, and transfection of ILK cDNA into the mutant cells increased not only ILK but also PINCH and α-parvin, resulting in the restoration of αIIbα6Bβ3 activation. In the parental cells expressing active αIIbα6Bβ3, ILK, PINCH, and α-parvin were co-immunoprecipitated, indicating the formation of the IPP complex. Moreover, short interfering RNA (siRNA) experiments targeting PINCH-1 or both α- and β-parvin mRNA in the parent cells impaired the αIIbα6Bβ3 activation as well as the expression of the other components of the IPP complex. In addition, ILK mutants possessing defects in either PINCH or parvin binding failed to restore αIIbα6Bβ3 activation in the mutant cells. Kindlin-2 siRNA in the parental cells impaired αIIbα6Bβ3 activation without disturbing the expression of ILK. For CHO cells stably expressing wild-type αIIbβ3 that is an inactive form, overexpression of a talin head domain (THD) induced αIIbβ3 activation and the THD-induced αIIbβ3 activation was impaired by ILK siRNA through a significant reduction in the expression of the IPP complex. In contrast, overexpression of all IPP components in the αIIbβ3-expressing CHO cells further augmented THD-induced αIIbβ3 activation, whereas they did not induce αIIbβ3 activation without THD. These data suggest that the IPP complex rather than ILK plays an important role and supports integrin activation probably through stabilization of the active conformation.

Citation: Honda S, Shirotani-Ikejima H, Tadokoro S, Tomiyama Y, Miyata T (2013) The Integrin-Linked Kinase-PINCH-Parvin Complex Supports Integrin αIIbβ3 Activation. PLoS ONE 8(12): e85498. doi:10.1371/journal.pone.0085498

Editor: Maddy Parsons, King's College London, United Kingdom

Received August 3, 2013; **Accepted** December 5, 2013; **Published** December 23, 2013

Funding: This work was supported in part by grants from the Ministry of Health, Labor, and Welfare of Japan; and from the Ministry of Education, Culture, Sports, Science, and Technology of Japan. The funders had no role in study design, data collection and analysis, decision to publish, or preparation of the manuscript.

Competing interests: The authors have declared that no competing interests exist.

* E-mail: shige@ncvc.go.jp

Introduction

Cell adhesions are critical for hemostasis processes composed of interactions between vessel walls, platelets and coagulation-related proteins. During these processes, cells react with several elements such as extracellular matrix (ECM) proteins and cell surface receptors. As one of the main elements, an integrin family is known to play a key role in cell-ECM interactions. Integrins, transmembrane glycoprotein adhesion receptors, are composed of α and β subunits and are linked non-covalently. Both subunits include long extracellular domains, transmembrane domains, and short cytoplasmic domains. There are at least two conformational states of integrin presenting low affinity (inactive) or high affinity (active) against its ligands and this heterodimeric receptor acts as a bidirectional signaling transducer. The binding of the cytoplasmic proteins such as talin and kindlins to the integrin β cytoplasmic domain upregulates the ligand-binding affinity of integrin (inside-out signaling). In contrast, ligand binding to integrins and the subsequent clustering of ligand-bound integrins result in intracellular molecular rearrangements such as focal adhesion formation and cell spreading (outside-in signaling) [1].

αIIbβ3, a major integrin expressed on platelets, is critical for platelet aggregation mediated by bindings of fibrinogen and von Willebrand factor. Since inside-out signaling pathways of αIIbβ3 induce striking conformational changes between inactive and active states, the activation processes of αIIbβ3 have been extensively investigated [2]. Talin, a cytoskeletal protein consisting of an N-terminal head and a C-terminal rod,